Available online at www.sciencedirect.com
ScienceDirect
Coordination Chemistry Reviews 250 (2006) 3161–3189
COORDINATION CHEMISTRY REVIEWS
www.elsevier.com/locate/ccr

Review

Anions as templates in coordination and supramolecular chemistry

Nélida Gimeno, Ramón Vilar*

Department of Chemistry, Imperial College London, London SW7 2AZ, UK

Received 28 March 2006; accepted 25 May 2006
Available online 3 June 2006

Contents

Abstract

This review aims to highlight the most important recent advances in the area of anion-templated syntheses in supramolecular and coordination chemistry. We published a comprehensive review on this area in 2003 and hence examples prior to this date will only be discussed when essential for clarity of presentation. The current review has been divided into three main sections: (a) anion-templated synthesis of systems with well-defined molecular weights; this includes macrocycles and cages, interlocked species (such as catenanes and rotaxanes), helical assemblies and other selected examples. (b) Anions as templates in polymeric systems; this includes metal-organic frameworks, molecularly imprinted polymers and other selected examples, such as liquid crystalline materials. (c) Anion templates in dynamic combinatorial libraries.

Keywords: Anion; Template; Macrocycles; Cages; Catenanes; Rotaxanes

1. Introduction

The use of chemical templates is now a well-established approach for the rational synthesis of molecular and supramolecular assemblies. As defined by Busch "*A chemical template organizes an assembly of atoms, with respect to one or more geometric loci, in order to achieve a particular linking of atoms*" [1]. This strategy, not only allows for the synthesis of molecules in a more efficient manner, but also to prepare assemblies that have unusual topologies, such as rotaxanes, helicates and catenanes [2]. Therefore, a templating agent can be said to *contain* the required information to organize a collection of building blocks so that they can be linked together in a specific manner.

As has been discussed in depth elsewhere [3], there are two types of templated processes: thermodynamic and kinetic. In the former, the template binds to one of the products (i.e. under thermodynamic control) shifting the equilibrium towards the formation of this product, which is hence obtained in high yields.

* Corresponding author. Tel.: +44 20 75941967; fax: +44 20 75941139.
E-mail address: r.vilar@imperial.ac.uk (R. Vilar).

0010-8545/$ – see front matter © 2006 Elsevier B.V. All rights reserved.
doi:10.1016/j.ccr.2006.05.016

In the case of kinetic templates, they operate under irreversible conditions stabilizing all the transition states that lead to the wanted product. In many of the kinetically controlled reactions, the template ends up strongly bound to the final species. In these cases it acts, not only as a kinetic template, but also as a thermodynamic one. In practice, it is often very difficult to unambiguously determine whether a templated reaction is kinetically or thermodynamically controlled. For the purposes of this review, a template (or directing agent) will be considered any species that organizes an assembly of molecular building blocks by non-covalent interactions favoring the formation of a specific product. The template can either be removed from the final product or kept as an integral part of it.

Although templated reactions have been known for many years, the use of anions as templates is still a relatively young area of research. In contrast to the widespread use of cationic templation, it is only over the past few years that negatively charged species have been successfully employed to direct the formation of specific molecules and assemblies. The slower development of this area (in comparison to cationic templates) has been partially attributed to the fact that anions have a diffuse nature, they are pH sensitive and have relatively high solvation free energies [4–6]. However, as has been demonstrated by the increasing number of anion-directed assemblies reported over the past 5 years, these *limitations* are not as critical as first thought.

This review aims to highlight the most important advances in the area of anion-templated syntheses in supramolecular and coordination chemistry over the past 3 years. A comprehensive review on this area was published by one of us in 2003 [7] and hence only examples prior to that date will be discussed when essential for clarity of presentation. The review has been divided into three main sections: (a) anion-templated synthesis of systems with well-defined molecular weights; this includes macrocycles and cages, interlocked species (such as catenanes and rotaxanes), helical assemblies and other selected examples. (b) Anion templates in polymeric systems; this includes metal-organic frameworks, molecularly imprinted polymers and other selected examples, such as liquid crystalline materials. (c) Anion templates in dynamic combinatorial libraries.

2. Anion-templated synthesis of systems with well-defined molecular weight

2.1. Anion-directed synthesis of macrocycles and cages

2.1.1. Macrocycles

Over the past 3 years, most of the developments in anion-templated syntheses of macrocycles (both organic and inorganic) have focused on studying in more detail previously reported systems. This has led to a better understanding of the templation process and also to exploiting anion-directed reactions for specific applications.

An efficient approach to assemble simple building blocks into large supramolecular aggregates is to use metal–ligand interactions. If these interactions are orchestrated by the appropriate template (e.g. an anion) a good level of control can be obtained

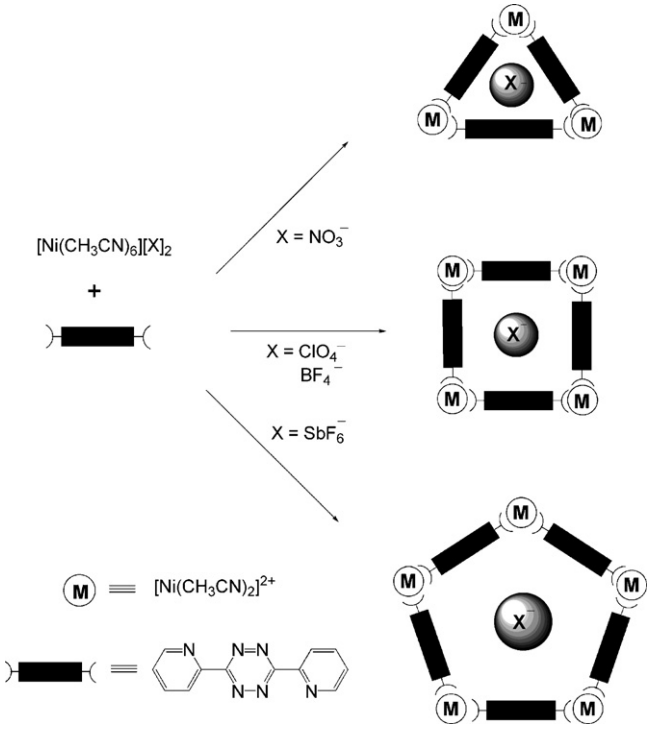

Scheme 1. Schematic representation of the anion-directed synthesis of metalla-macrocycles with different geometries.

over the geometry of the final assembly. An elegant example of this has been provided by Dunbar who has published a detailed study of the templating effect that a range of anions have in the formation of nickel(II) and zinc(II) metalla-cyclophanes using 3,6-bis(2-pyridyl)-1,2,4,5-tetrazine (bptz) as bridging ligand (see Scheme 1) [8]. Following up from their previous studies [9,10], this group has unambiguously demonstrated that anions, such as $[BF_4]^-$ and $[ClO_4]^-$, induce the formation of the tetrametallic square assemblies $[\{M_4(bptz)_4(CH_3CN)_8\}X][X]_7$ ($M = Zn^{II}$, Ni^{II}; $X = [BF_4]^-$, $[ClO_4]^-$), while the larger octahedral anion $[SbF_6]^-$ templates the formation of the molecular pentagon $[\{Ni_5(bptz)_5(CH_3CN)_{10}\}SbF_6][SbF_6]_9$.

The X-ray crystal structures of these species have shown that in both the squares (Fig. 1) and pentagon (Fig. 2) one anion is encapsulated at the centre of the corresponding metalla-cyclophane. Besides the fact that these anions pack efficiently in the cavity of the corresponding assembly, the X-ray structures provided evidence that there are anion–π interactions between the O/F atoms of the anions and the tetrazine rings of the bridging bptz ligand. This could be a determining factor in the ability of the anion to dictate the size of the metalla-macrocycle formed.

To investigate the stability of these assemblies these reactions were carried out with different ligand-to-metal ($M = Zn^{II}$ or Ni^{II}) ratios in the presence of the corresponding anion. These studies showed that the $[M_4]^{8+}$ cations readily form (in acetonitrile and at room temperature) regardless of the ratio of bptz to M^{II} salt (up to 10:1), indicating that their formation is highly favoured. Furthermore, there is no evidence of decomposition of the squares when they are refluxed in acetonitrile for up to 1 week. Similarly, the formation of the pentagon is also observed under various

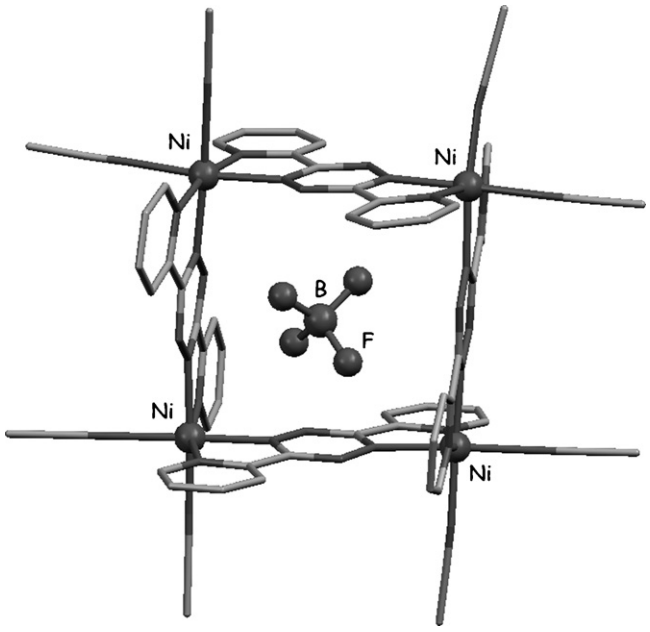

Fig. 1. Crystal structure of $[\{Ni_4(bptz)_4(CH_3CN)_8\}BF_4][BF_4]_7$ showing the encapsulated $[BF_4]^-$ anion.

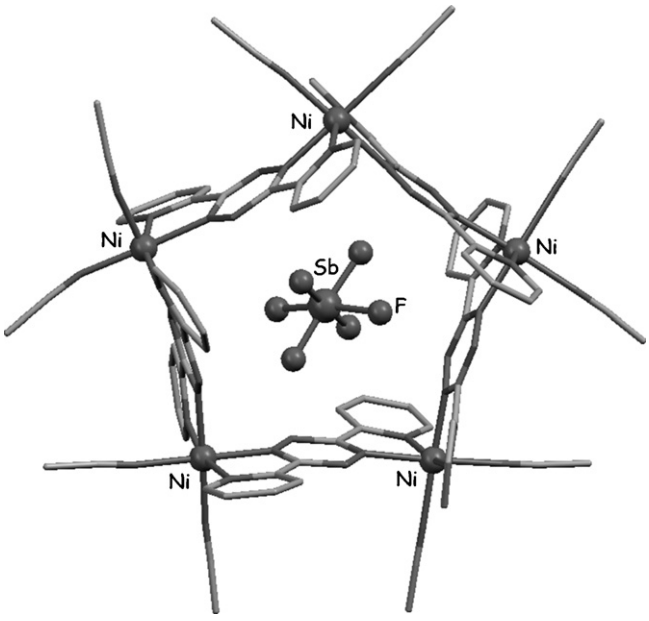

Fig. 2. Crystal structure of $[\{Ni_5(bptz)_5(CH_3CN)_{10}\}SbF_6][SbF_6]_9$ showing the encapsulated $[SbF_6]^-$ anion.

metal-to-ligand ratios (although the yields are lower if the stoichiometry is not the correct one); the pentameric structure is retained in acetonitrile even after refluxing for 1 week.

Interestingly, the analogous reaction to the ones described above between bptz and $Ni(NO_3)_2$ in acetonitrile yielded a product that, according to the spectroscopic characterisation, consists of a trimeric assembly (see Scheme 1). The same product is reported to form when treating the molecular pentagon with $[n\text{-}Bu_4N][NO_3]$. To date, no structural characterisation of this product has been reported.

The authors also investigated the possibility of converting one macrocycle to the other upon addition of the appropriate anion. Their results demonstrated that the molecular pentagon can be easily converted into molecular squares in the presence of excess $[BF_4]^-$ and $[ClO_4]^-$. Interestingly, the conversion of the molecular pentagon to the square is also observed upon addition of iodide; as the authors pointed out, the fact that a spherical anion can direct the formation of the square might seem contradictory to the idea that a specific shape of the anion is required for the formation of the corresponding macrocycle. However, if one considers the large size and polarizability of iodide, it is not unexpected that it can adopt the directionality of a tetrahedral anion.

In contrast to the above, the conversion of the nickel square to the corresponding pentagon in the presence of $[SbF_6]^-$ is not as favourable and only a part of it is transformed to the larger macrocycle. This apparently higher stability of the molecular square in comparison to the molecular pentagon can be attributed to the larger strain in the pentagon as is evident by the bending of the btpz ligands in its crystal structure.

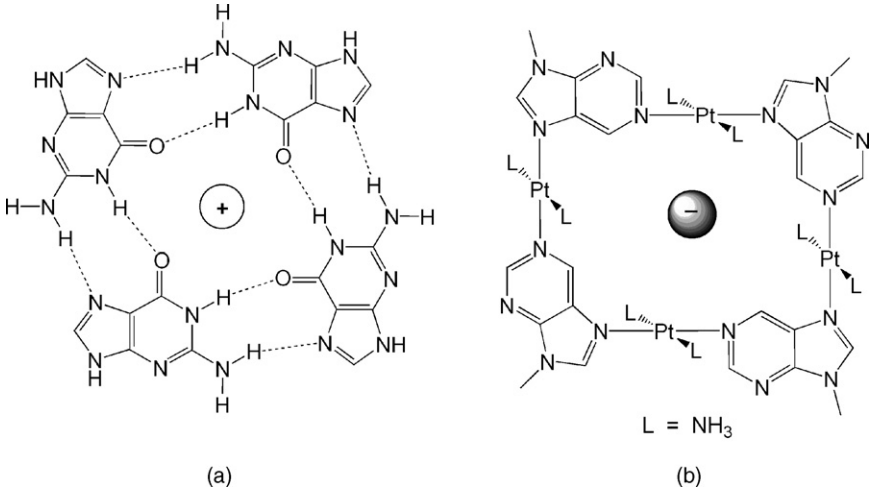

Fig. 3. Schematic representation of: (a) guanine-quartet with a cationic guest and (b) metalla-macrocycle **1** based on platinum(II) and methylpurine with an anionic guest.

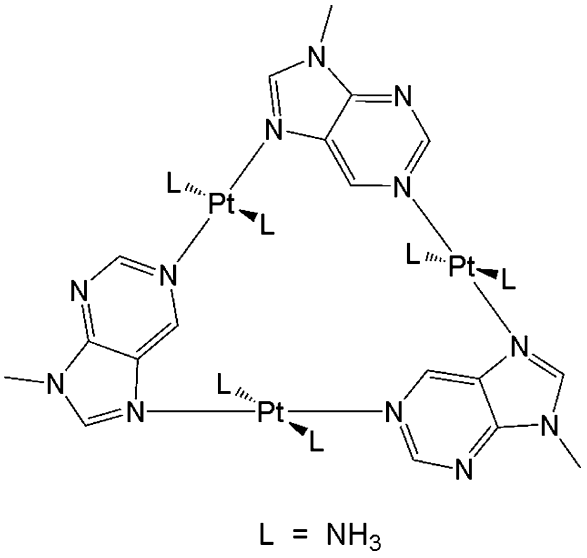

Fig. 4. Schematic representation of the molecular structure of the tri-platinum (II) complex **2**.

Hydrogen bonded guanine tetrads are important structural motifs in tetra-stranded DNA, which seems to play significant roles in the telomeres as well as in regulatory regions of the DNA [11]. In these tetrads (see Fig. 3a), the four guanine bases are interconnected by eight hydrogen bonds and they are stabilized by the presence of a cation at the centre of the square. Inspired by this natural motifs, Lippert has recently reported a tetrad that instead of using hydrogen bonds to interconnect purine bases, it employs platinum(II) centres (see Fig. 3b) [12].

The synthesis of square **1** was carried out by the self-assembly of four units of $[(NH_3)_2Pt(Pur)(H_2O)]^{2+}$ (where Pur = 9-methylpurine) over a period of 5 days. In the self-assembly process, a second species is formed with a triangular geometry (see Fig. 4). According to NMR experiments, the triangular species **2** is favoured (in a 0.6:1 ratio) to the square **1**. However, if the self-assembly process is carried out in the presence of $[SO_4]^{2-}$, the proportion of the two species changes (now the square is favoured over the triangle in a 2.5:1 ratio) and the reaction takes place in 3 instead of 5 days. This change in the preference for the square over the triangle has been attributed to the templating properties of the sulfate anion.

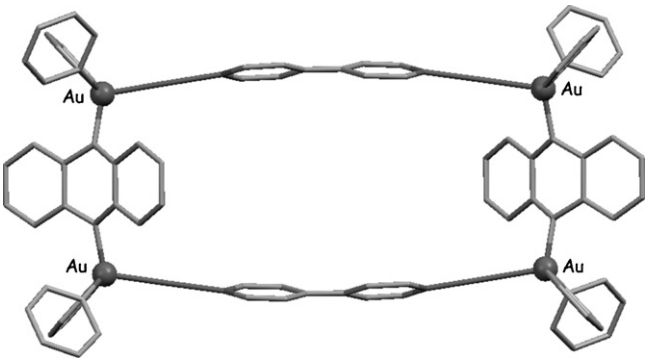

Fig. 5. Crystal structure of the luminescent gold(I) rectangle **3**.

Another example of anion-templated synthesis of metalla-macrocycles has been recently provided by Yip and co-workers [13]. This group has reported the synthesis and host–guest chemistry of a luminescent gold(I) molecular rectangle (**3**) (see Fig. 5). This complex is prepared by the sequence of reactions shown in Scheme 2, which involve the removal of chloride from the coordination sphere of the gold centres with $AgNO_3$ or $Ag(CF_3SO_3)$.

Interestingly, when this reaction is carried out using $AgBF_4$ or $AgClO_4$ to remove the chloride, the bipyridine-free tri-gold macrocycle **4** (see Fig. 6) is formed instead. This species had been previously reported by the same authors [14] and was prepared directly from refluxing a solution of the phosphine with $Au(Me_2S)Cl$ followed by addition of $LiClO_4$.

The X-ray structure of this tri-gold assembly shows that one of the anions is positioned at the centre of the metalla-macrocyle with its oxygen atoms directed to the centre of the anthracene rings of the bridging phosphine. Although no further evidence has been provided to demonstrate the potential templating role of the anions, it is likely that they exert an important influence in determining the size and assembly of the macrocycles obtained. Future studies should be carried out to investigate the nature of the products resulting from the reaction between equimolar mixtures of the phosphine, $Au(Me_2S)Cl$ and other AgX salts (including CF_3SO_3 and NO_3).

When studying the ability of anions to direct the formation of a specific metalla-assembly, it is often difficult to separate those effects that are purely due to templation (as those dis-

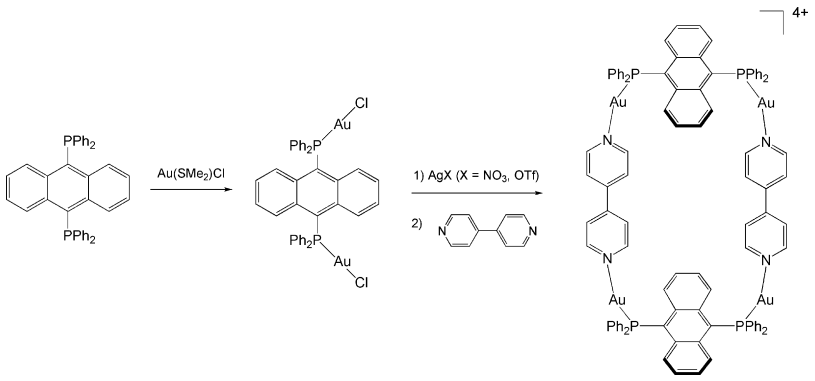

Scheme 2. Synthetic procedure for the preparation of **3**.

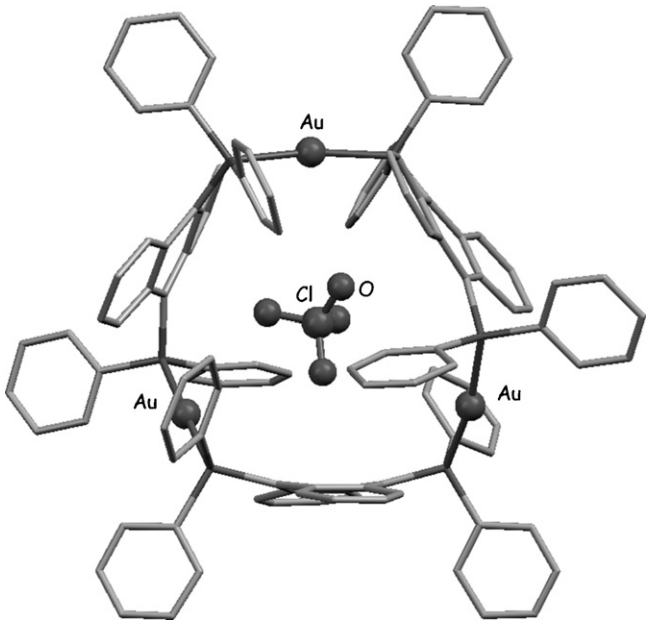

Fig. 6. Crystal structure of the tri-gold(I) macrocycle **4**.

cussed above) from those that are a consequence of the different coordinating capabilities of specific anions. An example of this are a series of silver(I) complexes with 1,3-bis(benzimidazol-1-ylmethyl)benzene (**5**) reported by Amouri and co-workers [15]. More specifically, the reaction between AgX ($X = NO_3$, CF_3SO_3) and **5**, yields the metalla-macrocycles $[Ag_2(\mathbf{5})_2]X_2$ shown in Fig. 7. The crystal structure of one of these metalla-macrocycles (with $X = CF_3SO_3$) revealed that the anions are directly coordinated to the metal centres.

However, when the reaction is performed under the same conditions but using $AgBF_4$, the formation of an infinite coordination network is observed. In this polymeric assembly, the anions are not interacting directly with the silver(I) centres (see Fig. 8).

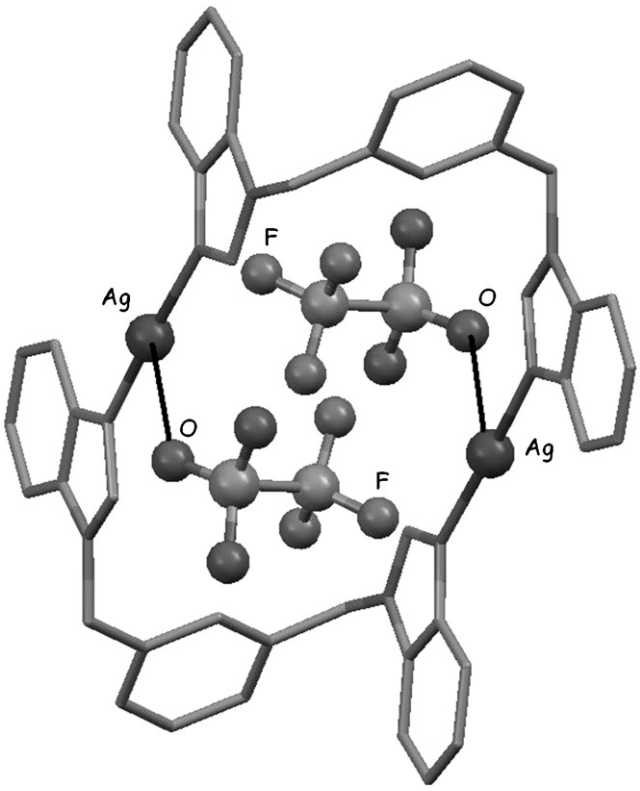

Fig. 7. Crystal structure of the silver(I) macrocycle $[Ag_2(\mathbf{5})_2](CF_3SO_3)_2$.

Similarly, Bu and co-workers have reported that the reactions of various copper(II) salts with 2,5-bis(3-pyridyl)-1,3,4-oxadiazole ($\mathbf{L^1}$) yield very different products depending

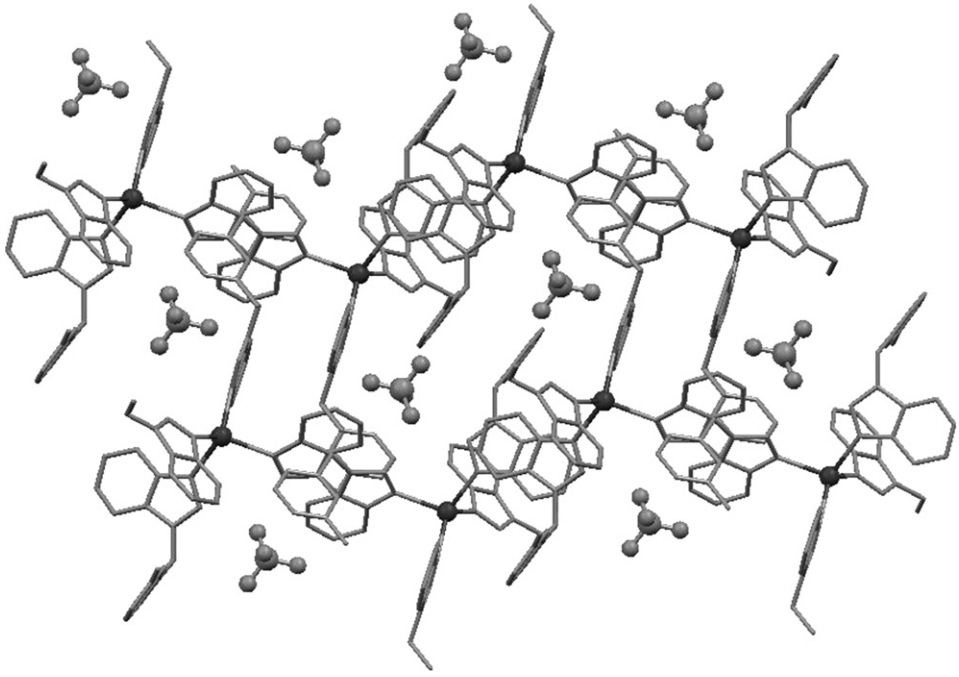

Fig. 8. Crystal structure of the infinite coordination network resulting from the reaction between $AgBF_4$ and ligand **5**.

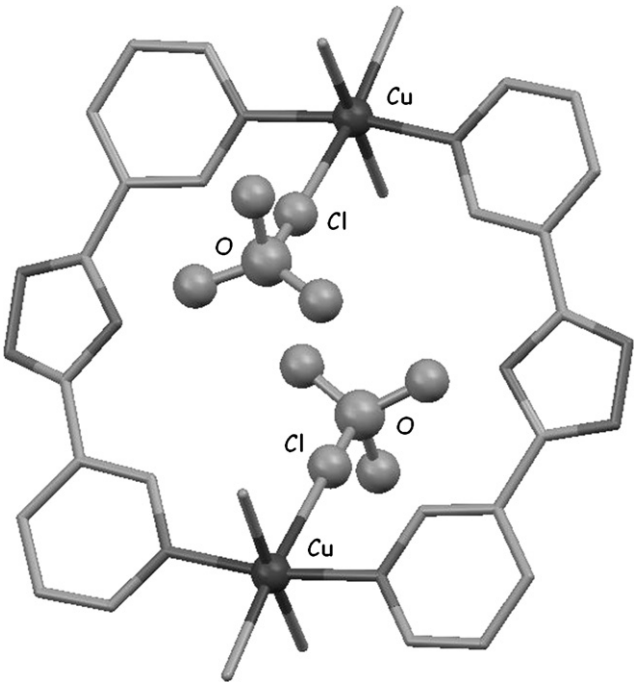

Fig. 9. Crystal structure of complex **6** showing the interaction between the copper(II) centres and two of the perchlorate anions.

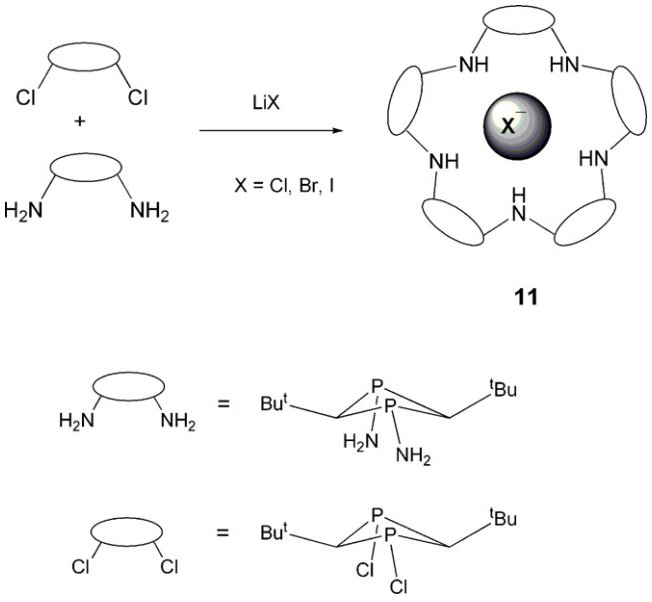

Scheme 3. Schematic representation of the synthesis of the halide-templated synthesis of macrocycle **11**.

on the nature of the copper salt's counterion [16]. When $Cu(ClO_4)_2$ or $Cu(NO_3)_2$ are employed the metalla-macrocycles $[Cu_2(\mathbf{L^1})_2(H_2O)_6][ClO_4]_4$ (**6**) and $[Cu_2(\mathbf{L^1})_2(NO_3)_4]$ (**7**) are obtained (see Fig. 9 for the X-ray crystal structure of **6**). In contrast, when $CuSO_4$ or $Cu(OAc)_2$ are used, two different one-dimensional (1D) polymeric assemblies (X = SO_4, **8**; X = OAc, **9**) are formed (see Fig. 10).

The role of the anions in these systems is clearly very important. While in the metalla-macrocycle **6**, $[ClO_4]^-$ simply acts as a counter-anion balancing the electrostatic charge, in the analogous compound **7** the nitrate anions are directly coordinated to the metals. In the 1D coordination polymers **8** and **9**, the counteranions interact with the metal centres, in **8** each sulfate is bound to one copper while in the structure of **9** the acetate bridge two metal centres forcing the ligands to bind in a *trans* disposition (generating a zigzag type structure). As the authors point out, the steric bulk and shape of the anions studied might also play an important role in directing the formation of a specific assembly.

Besides the extensive use of metal–ligand interactions to prepare different sized macrocycles, there are several examples where anions template the formation of covalently linked cyclic species. For example, Wright and co-workers reported in 2003 the halide-templated synthesis of a series of macrocycles containing $[\{P(\mu\text{-}N\mathit{t}Bu)_2\}(\mu\text{-}NH_2)]_n$ frameworks [17]. These macrocyclic species were synthesized from the reaction between $[ClP(\mu\text{-}N\mathit{t}Bu)]_2$ and $[NH_2P(\mu\text{-}N\mathit{t}Bu)]_2$ in the presence of a base. When this reaction is carried out in THF/NEt_3 the major product is the tetrameric species $[\{P(\mu\text{-}N\mathit{t}Bu)_2\}(\mu\text{-}NH_2)]_4$ (**10**) but when the same reaction is carried out in the presence of an excess of LiCl the tetramer formation is suppressed and the synthesis of the pentamer $[\{P(\mu\text{-}N\mathit{t}Bu)_2\}(\mu\text{-}NH_2)]_5(HCl)]$ (**11**) is favoured (see Scheme 3). Structural characterisation of this pentamer has shown that the chloride is positioned at the centre of the macrocycle interacting with the NH groups of the ring via hydrogen bonds.

More recently, it has been demonstrated that the pentamer can also be templated by bromide and iodide [18]. For example, the use of LiI yielded the pentamer in a 44%. ^{31}P NMR spectroscopic studies have shown that the ability of the halides to template the formation of the pentamer follow the order $I^- > Br^- > Cl^-$. These investigations have also revealed that the two macrocycles (**10** and **11**) are not in a dynamic equilibrium

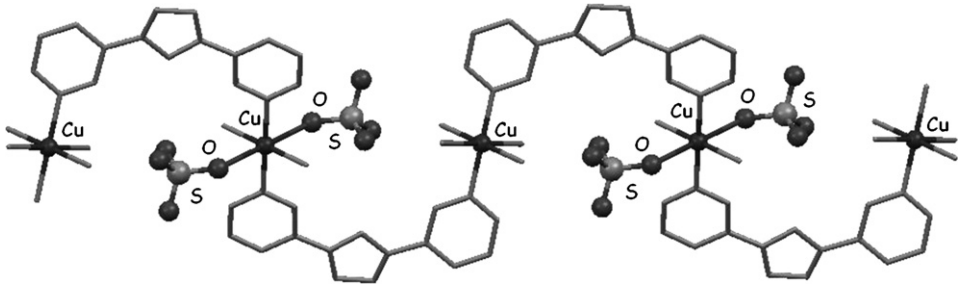

Fig. 10. Crystal structure of the coordination polymer **8** showing the interaction between the anion and the metal centres.

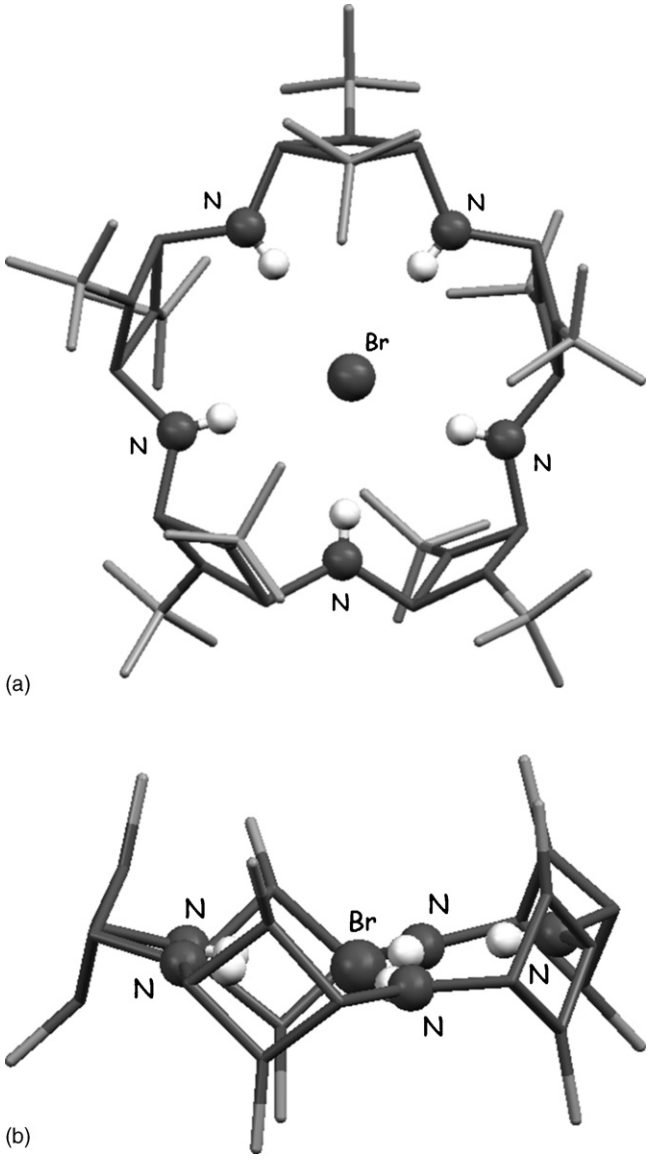

Fig. 11. Two different views of the crystal structure of macrocycle **11**·(HBr). As can be seen on the bottom structure, the bromide is located inside the macrocycle.

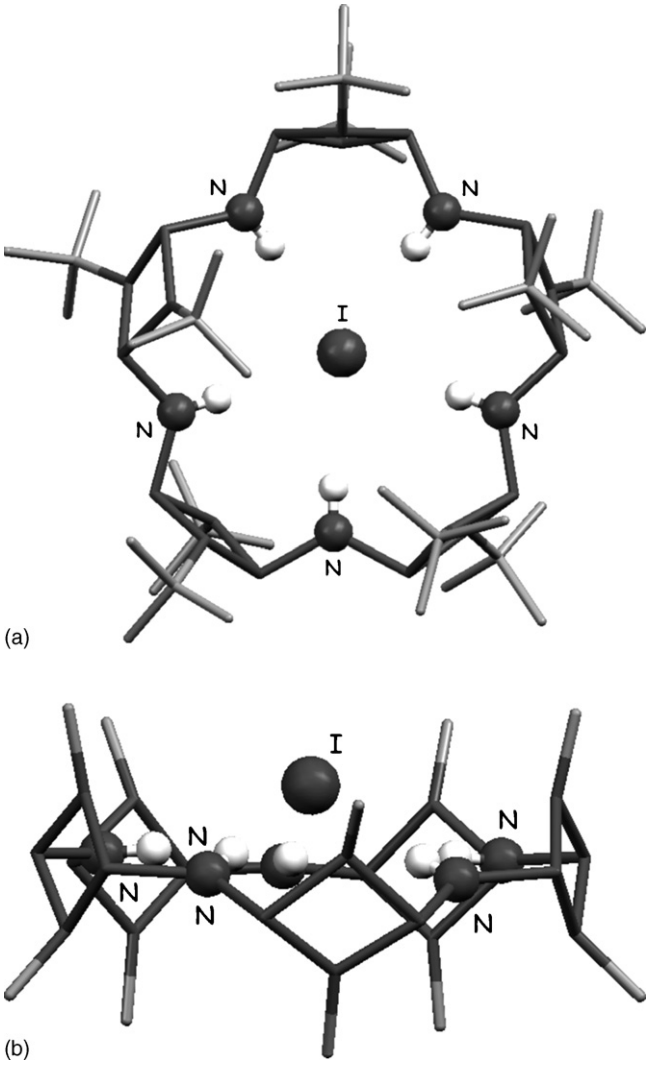

Fig. 12. Two different views of the crystal structure of macrocycle **11**·(HI). As can be seen on the bottom structure, the iodide is located above the plane formed by the macrocycle.

with each other, suggesting that their formation is kinetically rather than thermodynamically controlled.

In their most recent study [18], Wright and co-workers report the crystal structures of the pentamers with encapsulated bromide and iodide (see Figs. 11 and 12). An interesting aspect of the iodide-templated macrocycle is that, in contrast to the chloride and bromide analogues, the anion sits 1.36 Å above the plane of the ring. This is clearly due to the larger size of iodide in comparison to the other halides.

The structural data obtained for the three assemblies, suggests that the least thermodynamically stable host–guest complex is that one with iodide. This is surprising since this anion is the one that acts as the best template for the cyclisation reaction to yield the pentamer. To support these structural observations, the same authors have reported a computational study which confirms that the thermodynamic stabilities of model host–guest species are in the order $Cl \approx Br > I$, which is indeed the reverse of the templating trend observed experimentally. These observations support the proposition that the formation of this cyclic species is an example of a kinetically controlled anion-templated reaction.

Other examples of anion-templated synthesis of covalently linked macrocycles have been provided by Alcalde and co-workers [19]. This group previously reported the halide-directed synthesis of a series of [1_4] imidazoliophanes (Scheme 4) [20]. Recently, they have extended these studies to evaluate quantitatively the templating effect of halides, in particular of chloride, in the formation of the macrocycles. The methodology used to prepare these cyclic structures is based on a "3 + 1" convergent synthesis taking place in two steps (see Scheme 4).

The preparation of the reaction intermediate **12** allowed the authors to evaluate the kinetics of the ring-closure reaction in the presence and absence of the templating chloride. These studies provided clear evidence of the templating effect exerted by chloride since addition of [Bu_4N]Cl to the reaction mixture increased the ring-closure of **12** up to 10 times.

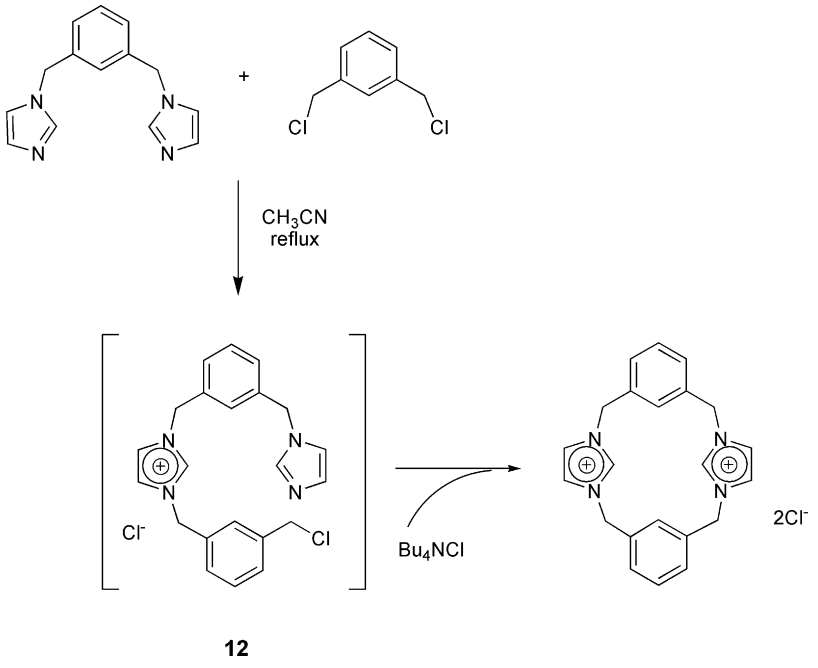

12

Scheme 4. Schematic representation of the chloride-templated synthesis of [1_4] imidazoliophanes.

Over the past few years, Sessler has studied the effect that anions have in the synthesis of various macrocycles [21]. Recently, he has reported the anion-induced synthesis of new bipyrrole-based macrocyclic receptors [22]. The reaction of diamine **13** (see Scheme 5) and diformylbipyrrole (**14**) was performed in different acidic media and, depending on the acid used (namely HCl, HBr, CH_3CO_2H, CF_3CO_2H, H_3PO_4, H_2SO_4 or HNO_3), different distributions of oligomeric species and macrocycles were obtained. However, when sulfuric acid was employed, the [2 + 2] macrocycle **15**·$2H_2SO_4$ was formed in nearly quantitative yield (see Scheme 5).

When **15**·$2H_2SO_4$ was treated with triethylamine in dichloromethane the anion-free macrocycle **15**, was isolated in 75% yield and its solid state structure determined by X-ray crystallography. This macrocycle was then titrated with different anions showing strong interactions with tetrahedral anions, such as dihydrogenphosphate and sulfate (with association constants in acetonitrile of $107{,}000 \pm 9600$ and $63{,}500 \pm 3000\ M^{-1}$, respectively).

Interestingly, when **15** was allowed to stand in acetonitrile for 5 days in the presence of sulfate or dihydrogenphosphate, it rearranged to give the [3 + 3] macrocycle **16** (see Fig. 13) in 47% yield (for sulfate) and quantitative yield (for $H_2PO_4^-$).

The formation of this (larger) macrocycle in the presence of specific anions, suggests that a dynamic equilibrium between various species is present and the addition of a specific template amplifies the formation of one of them. As will be discussed in Section 4 of this review, dynamic combinatorial approaches

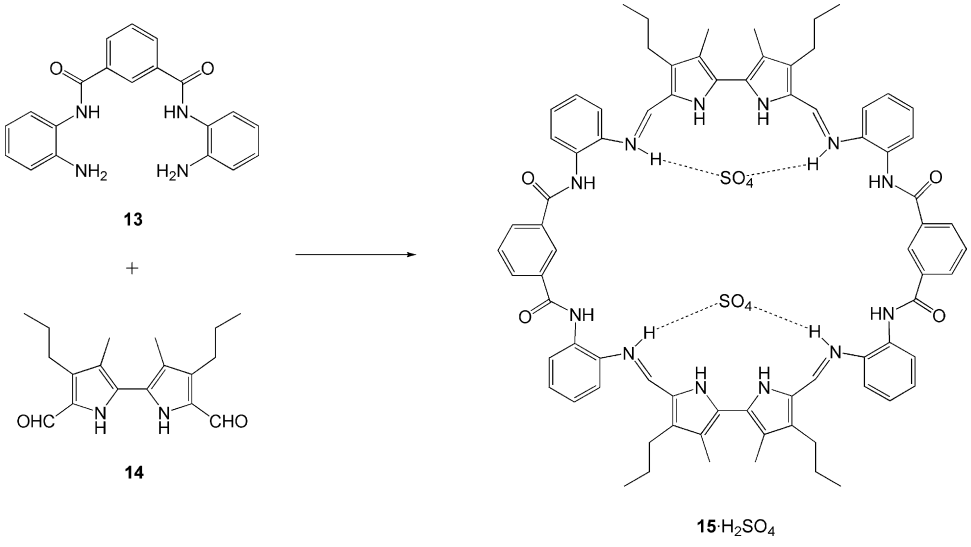

13 + **14** → **15**·H_2SO_4

Scheme 5. Reaction scheme for the synthesis of the macrocycle **15**·H_2SO_4.

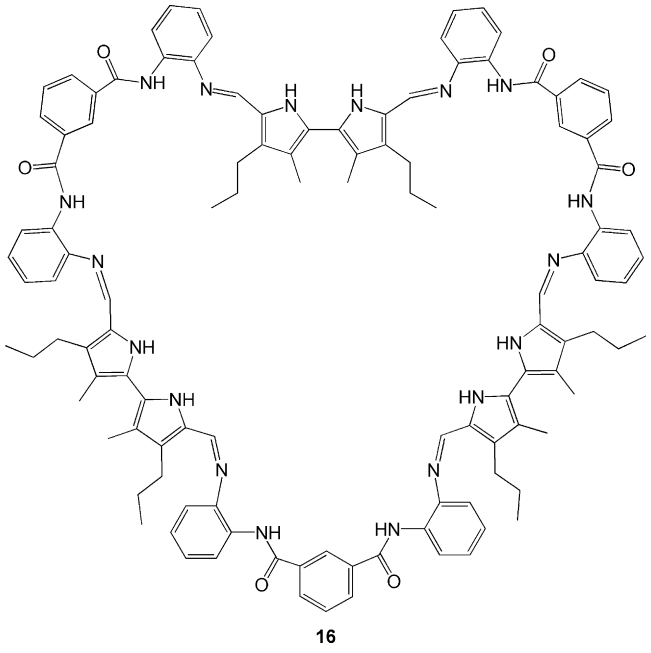

16

Fig. 13. The larger macrocycle **16** forms when the reaction is left to stand for long periods of time.

make use of this principle (i.e. modification of the equilibrium upon addition of a template) for the synthesis of selective receptors.

2.1.2. Anion-templated synthesis of cages and capsules

As has been shown in the previous section, in an anion-templated process, there are several potential non-covalent interactions that can be employed to direct the reaction. Some of these interactions involve hydrogen-bonding between the anion and the building blocks to be assembled, weak metal···anion interactions, anion···π contacts or simply electrostatic attraction between the anion and positively charged species. Several of these interactions have been shown to play an important role in the synthesis of the metal-containing macrocycles and cages shown in Scheme 6. These species were first reported [23,24] in the late 1990's and several studies followed to unambiguously establish the templating role of halides in the formation of the metalla-assemblies [25,26].

The reaction between six equivalents of $NiCl_2$ and eight equivalents of amidinothiourea (Hatu) in methanol yields the dark-green hexa-nickel cage $[Ni_6(atu)_8Cl][Cl]_3$ ($[\mathbf{17}][Cl]_3$). In contrast, when the same reaction is repeated using other nickel sources, such as NiX_2 (where $X = Br^-$, I^-, $[AcO]^-$, $[NO_3]^-$, $[ClO_4]^-$) the simple square planar orange compound $Ni(atu)_2$ (**18**) is formed, instead of the corresponding cage (see Scheme 6).

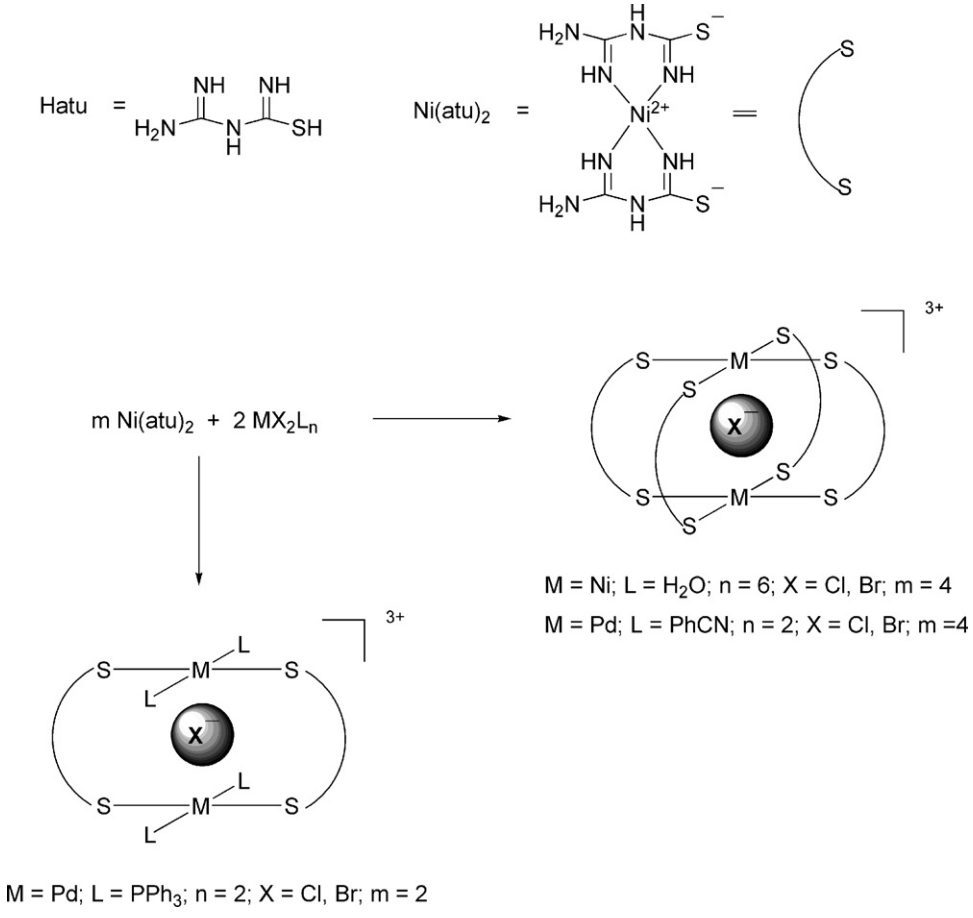

Scheme 6. Reaction scheme showing the synthesis of different metalla-cages (for example, **17**) and macrocycles using $Ni(atu)_2$ (**18**) as building block.

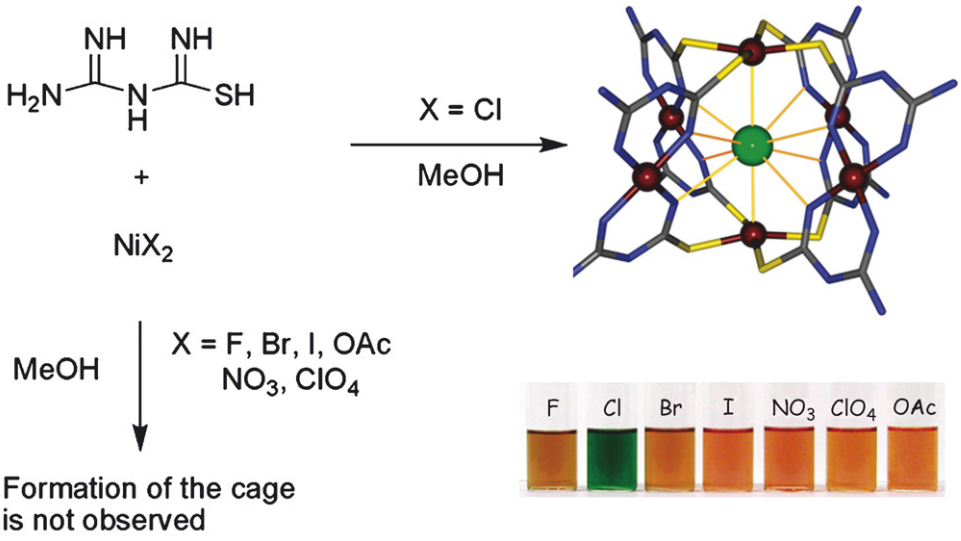

Fig. 14. The chloride-templated synthesis of metalla-cage **17** (upper right corner of the figure) is associated with a colour change (from orange to green), which has been used as a colorimetric way of detecting chloride anions in methanolic solution. (For interpretation of the references to colour in this figure legend, the reader is referred to the web version of the article.)

Addition of chloride to any of these mixtures induces the formation of the cationic cage $[\mathbf{17}]^{3+}$ (with an encapsulated chloride and three external counterions). The formation of this cage is associated to a colour change from orange (from the $Ni(atu)_2$ square planar building blocks) to dark-green (from the cage). Recently, this colour change has been successfully exploited to develop a chemical sensor for the quantitative detection of chlorides in solution (see Fig. 14) [27]. This is one of the very few examples in which an anion-templated process has been employed as means to detect the presence of an anionic analyte (the template itself) in solution.

Bidentate pyrazolyl-based ligands have shown to be versatile building blocks for the synthesis of a wide range of coordination assemblies. Amongst the complexes that can be formed, McCleverty and co-workers reported in the late 1990's the synthesis of cages $[Co_4(\mathbf{L}^n)_6(X)][X]_7$ (where $\mathbf{L^2}$ and $\mathbf{L^3}$ = bidentate pyrazolyl-pyridine ligands; X = $[BF_4]^-$, $[ClO_4]^-$; see Fig. 15) and proposed that the encapsulated anion had a templating role [28]. Further to their initial findings, the authors carried out more detailed investigations of the assembly process in solution and demonstrated by NMR spectroscopy that indeed the tetrahedral $[BF_4]^-$ and $[ClO_4]^-$ act as templating agents for the formation of the tetrahedral cages [29].

In a more recent paper, Ward and co-workers have also explored the effect that the length of the ligand has on the formation of the cages [30]. When $\mathbf{L^4}$ was used as a bidentate ligand (see Fig. 16), the expected $[Co_4(\mathbf{L^4})_6(X)][X]_7$ (X = $[BF_4]^-$, $[ClO_4]^-$, $[PF_6]^-$, I^-) cages were formed but in this case the role of the anion is not as important as in the formation of the cages with the shorter ligands. As indicated by the authors, the assembled cage is sufficiently large to leave gaps in the centre of the faces through which the encapsulated anion can easily exchange with the external anions.

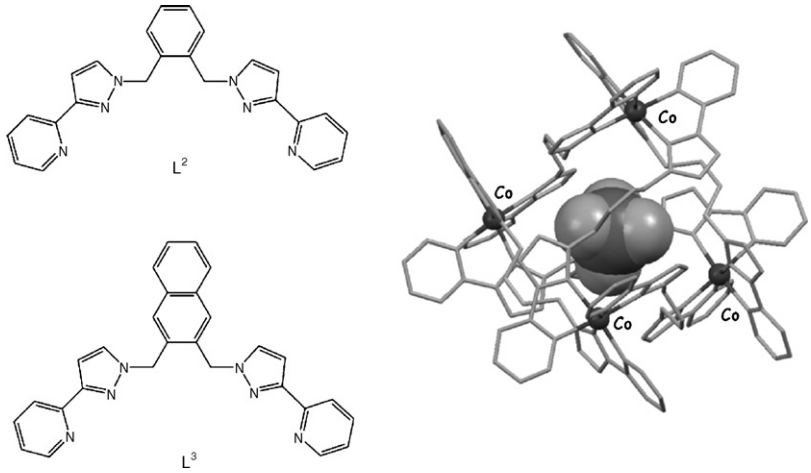

Fig. 15. Schematic representation of ligands $\mathbf{L^2}$ and $\mathbf{L^3}$, and crystal structure of $[Co_4(\mathbf{L^2})_6(ClO_4)][ClO_4]_7$ showing the tightly encapsulated anion (the bridging ligands have been simplified for clarity).

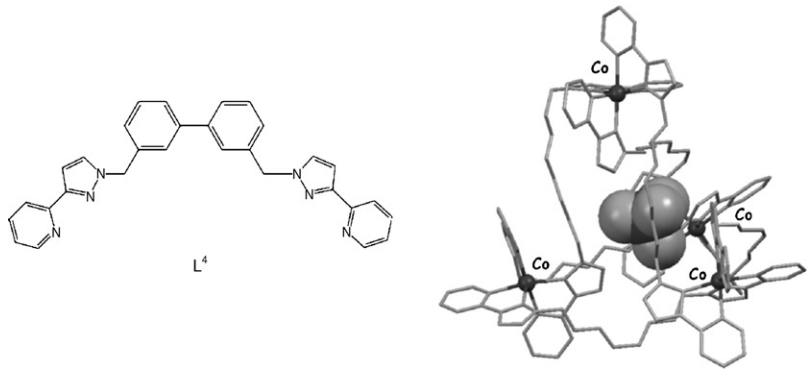

Fig. 16. Schematic representation of the longer ligand $\mathbf{L^4}$ and crystal structure of $[Co_4(\mathbf{L^4})_6(BF_4)][BF_4]_7$ showing the encapsulated anion.

Using the ligand shown in Fig. 17, Amouri et al. have recently reported the synthesis of the coordinatively unsaturated metallacages $[Co_2(\mathbf{L^5})_4(RCN)_2(BF_4)][BF_4]_3$ (R = Me, Et, Ph) [31]. The X-ray crystal structure of this assembly (see Fig. 17) has revealed that, as in the cages previously reported by McCleverty and Ward, the tetrahedral anion is encapsulated at the centre of the cage. In these species, there is a direct interaction between the coordinatively unsaturated cobalt(II) centres and the encapsulated $[BF_4]^-$ anion. Although in this work, the effect of other anions in the formation of the cage was not reported, considering the results previously obtained by McCleverty and Ward and the current evidence obtained by Amouri, it is likely that this tetrahedral anion is indeed templating the formation of the metalla-assembly.

Anions have also been found to be good templates in the formation of large poly-oxometallic systems. In the early 1990s, Müller et al. reported several examples where anions, such as nitrate and halides controlled the aggregation of $V^{n+}O_x$ polyhedra into cage type structures, such as $[HV_{18}O_{44}(NO_3)]^{10+}$ (**19**), $[H_4V_{18}O_{42}Br]^{9+}$ (**20**) and $[HV_{22}O_{54}(SCN)]^{6+}$ (**21**) [32]. It was shown that the size of the anion dictates the structure and geometry of the products obtained. More recently, Müller et al. have reported several more nano-scale objects where anions (in particular $[SO_4]^{2-}$) play an important role in defining their geometry and size. For example, the species $[Mo^{VI}_{114}Mo^{V}_{32}O_{429}(H_2O)_{50}(KSO_4)_{16}]^{30-}$ (**22**) comprises a molybdenum-based wheel-shaped host, encapsulating 16 K^+ and $[SO_4]^{2-}$ ions [33]. These ions form an unusual 64-membered $\{K(SO_4)\}_{16}$ ring inside the metalla-host (see Fig. 18).

The nano-sized host:guest complex was obtained when high concentrations of K_2SO_4 were present in a reaction mixture

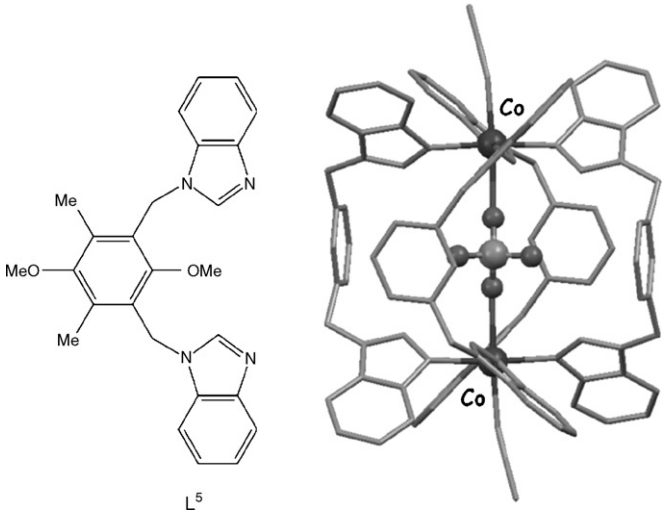

Fig. 17. Schematic representation of ligand $\mathbf{L^5}$ and crystal structure of $[Co_2(\mathbf{L^5})_4(MeCN)_2(BF_4)][BF_4]_3$ showing the encapsulated anion.

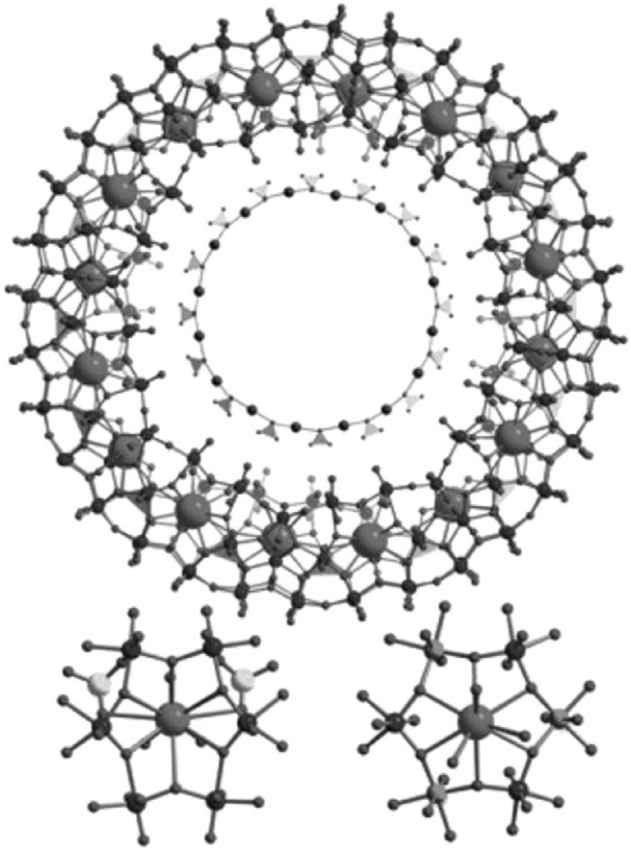

Fig. 18. Crystal structure of **22** highlighting the K^+ centres (larger spheres) and SO_4^{2-} anions (polyhedral representation). The interaction of K^+ with one $\{Mo_6O_6\}$ unit is shown at the bottom left of the figure. In order to show more clearly the $K^+SO_4^{2-}$ interactions, the structure of the $\{K(SO_4)\}_{16}$ ring is presented on a smaller scale and removed from its environment at the centre of the crystal structure (figure taken from *Chem. Commun.* (2003) 2000 [33]—reproduced by permission of The Royal Society of Chemistry).

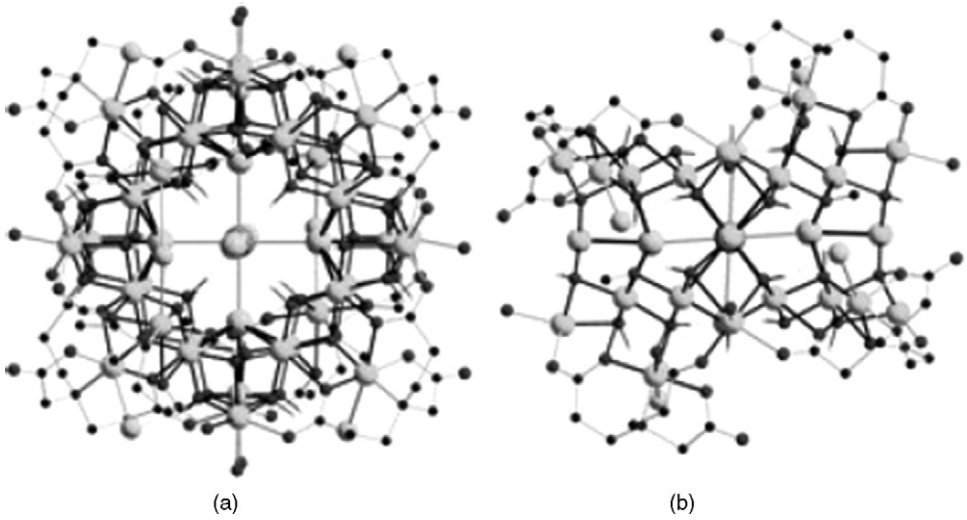

Fig. 19. Two views of the crystal structure of the Cu_{36} aggregate reported by Powell and co-workers [34] in which an encapsulated $[KCl_6]^{5-}$ has been proposed to act as a template (figure taken from *Chem. Comm.* (2004) 1598—reproduced by permission of The Royal Society of Chemistry).

known to form mixtures of discrete wheel-shaped species. Considering the inclusion of both ions inside the molybdenum-based host and their interaction with the external wheel, they apparently play a templating role in the formation of this specific nano-wheel.

Other examples of large metallic assemblies influenced by the presence of anions are the Cu_{36}^{II} and Cu_{44}^{II} aggregates recently reported by Powell and co-workers. These large assemblies are prepared by mixing copper(II) salts with aminopolycarboxylates in aqueous or alcoholic solvents. More specifically, a mixture of (nitrilodipropionic)acetic acid, KOH and $CuCl_2$ in methanol yielded crystals of the Cu_{36} aggregate shown in Fig. 19 [34]. Interestingly, this structure contains a $[KCl_6]^{5-}$ anion at its centre which is proposed to act as an scaffold to assemble 28 of the 36 copper(II) centres. In the presence of other anions, the same process leads to the formation of different structures.

Recently, the same authors reported the formation of a Cu_{44} aggregate (see Fig. 20) when (nitrilotripropionic)acetic acid, CsOH and $CuBr_2$ were mixed in water [35]. In this assembly, the two μ_8-bromide anions play an important directing role in the formation of this unusually large copper aggregate.

In all the examples discussed so far, the templating anion directs the formation of a specific assembly by pre-organizing the building blocks around it. However, there are systems in which anions act as "external" templates organizing the building blocks by interacting with the surface of the assembly. An early example of this is the hexa-silver cage reported by James and Mingos, which is templated by anions, such as triflate and nitrate [36,37]. A more recent example where an anion acts as an "external" template is the mixed-metal organometallic assembly reported by Tessier and co-workers [38]. The reaction between the tripodal rhodium phenylacetylide and $AgBF_4$ yields the Ag_2Rh_2 complex **23** in which BF_4 act as counterions only (see Scheme 7 and Fig. 21).

However, when the analogous reaction is carried out with $Ag(CF_3SO_3)$ the formation of complex **24** is observed instead.

In contrast to **23**, compound **24** contains only one tripodal rhodium phenylacetylene unit, which brings together three silver atoms. Interestingly, the X-ray structure of this assembly revealed that one of the three triflate anions interacts with the

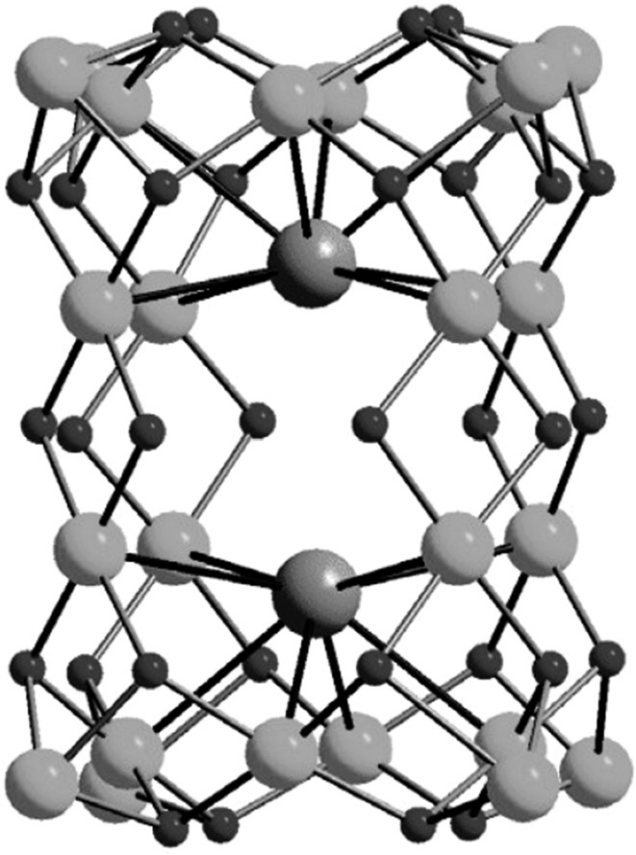

Fig. 20. Crystal structure of the inorganic $[Cu_{24}(\mu_8\text{-}Br)_2(\mu_3\text{-}OH)_{24}(\mu\text{-}OH)_8]^{14+}$ of the Cu_{44} aggregate reported by Powell and co-workers [35] (figure taken from *Inorg. Chem.*43 (2004) 7269—reproduced by permission of The American Chemical Society).

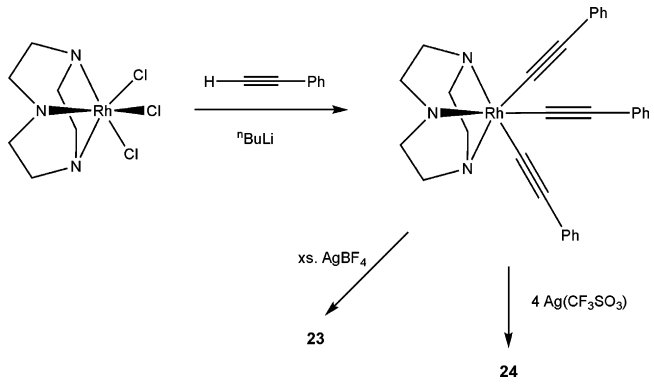

Scheme 7. Reaction scheme for the synthesis of the rhodium complexes **23** and **24**.

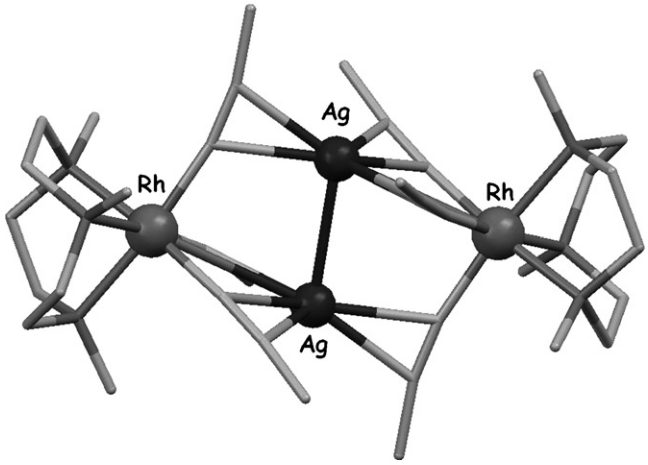

Fig. 21. Crystal structure of the tetra-metallic complex **23**.

three silver atoms directing the formation of the tripodal assembly (see Fig. 22).

2.2. Helical structures

There are only a handful of examples where anion-directed approaches have been employed for the assembly of metal-free helices. The first examples were reported by de Mendoza and co-workers (using sulfate anions and oligo-guanidinium strands) [39] and some years later by Kruger and co-workers (who employed chlorides to assemble pyridinium-containing ligands) [40]. More recently, Gale and co-workers have reported the first example of an anion-templated assembly of a helix formed

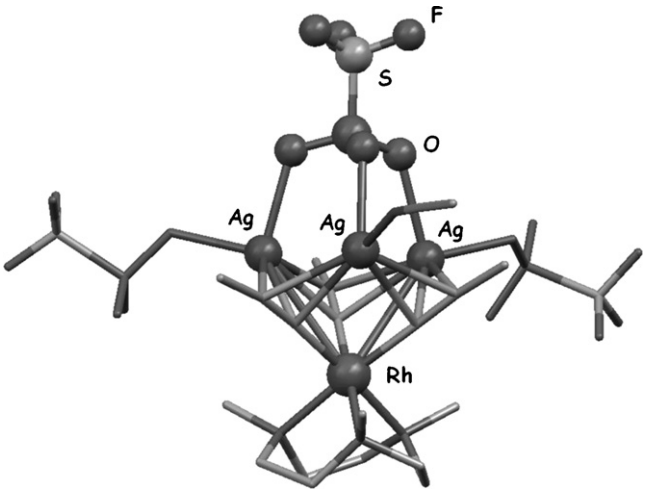

Fig. 22. Crystal structure of the tetra-metallic complex **24** showing the interaction of the triflate anion with the three silver(I) centres.

by two neutral strands (containing amides as hydrogen bond donors) [41]. More specifically, fluoride anions were shown to direct the assembly of two isophthalimide-containing strands into a double helix. An X-ray crystal analysis of this assembly (see Fig. 23) showed the formation of the helical structure around two fluoride anions via N–H···F hydrogen-bonding, as well as by π–π interactions of the terminal nitroaromatic rings. ^{1}H NMR spectroscopic studies were carried out in solution being consistent with the formation of a 2:2 assembly.

2.3. Interlocked assemblies

Traditionally, the preparation of molecular interlocked systems has been achieved by templation with cationic or neutral species through hydrogen-bonding, π–π stacking interactions, metal–ligand coordination and solvophobic interactions [42–52]. In contrast, until recently there were practically no examples reported of the use of anions as templates for the synthesis of this type of interlocked systems.

The first examples of interlocked species synthesized by anion-templated approaches were the pseudorotaxanes and rotaxanes reported in the late 1990's by Stoddart and co-workers [53,54] and Vogtle and co-workers [55,56]. More recently, Beer and co-workers have developed a methodology for the anion-templated synthesis of a wider range of interlocked species based on coupling the recognition of halides by a hydrogen-bonding

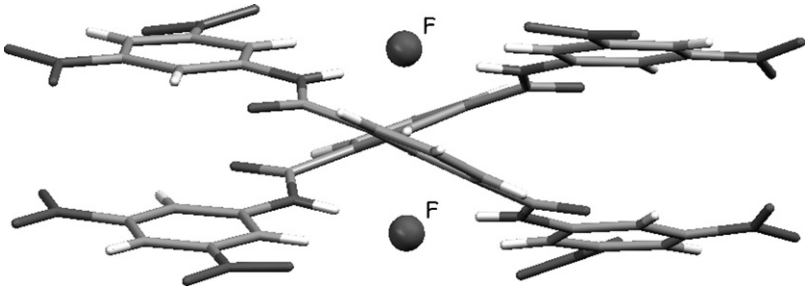

Fig. 23. Crystal structure of the helicate formed by two isophthalimide-containing strands positioned around two templating fluoride anions.

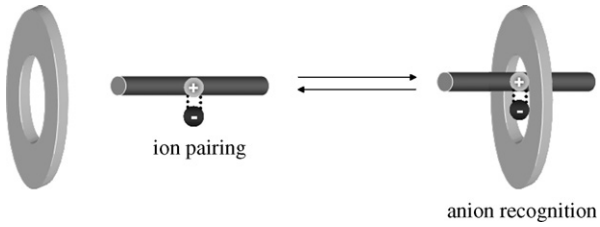

Fig. 24. Schematic representation of the anion-templated synthesis of interlocked species developed by Beer and co-workers [57].

host (e.g. a macrocycle) with ion-pairing between the corresponding halide and a second cationic species [57,58]. These two interactions provide the driving force for interpenetration, which can then yield the corresponding interlocked assembly (see Fig. 24).

Different sized isophthalamide-macrocycles containing polyether functionalities were designed to act as the wheel through which a cationic species could thread forming a [2]-pseudorotaxane. Molecules containing groups, such as pyridinium, imidazolium, benzimidazolium and guanidinium derivatives, were used as the cationic threads (see Scheme 8).

The assembly of pseudorotaxanes was achieved in all cases and was confirmed by single-crystal X-ray analysis as well as ^{1}H NMR studies [59]. These studies have indicated the important templating role of the anion (chloride showing to be the optimum template). The importance of the ion-pairing has also been investigated showing that strongly bound assemblies were formed in the case of the pyridiniun-based systems, while weaker ones were obtained with imidazolium and guanidinium threads.

An analogous strategy to the above but including a "clipping" step, was employed for the formation of rotaxanes [60]. In this case, the thread also included two stoppers while the precursor of the wheel contained two allylic end groups that could allow the closing of the rotaxane by a simple olefin metathesis reaction using Grubbs' catalyst (see Fig. 25).

Formation of the rotaxane in a 47% yield was achieved with compounds **25** and **26** in the presence of chloride (see Scheme 9). Interestingly, when the same reaction was carried out in the presence of hexafluorophosphate no interlocked product was detected.

Formation of the rotaxane – when using chloride as template – was confirmed by ^{1}H NMR spectroscopy. Large downfield

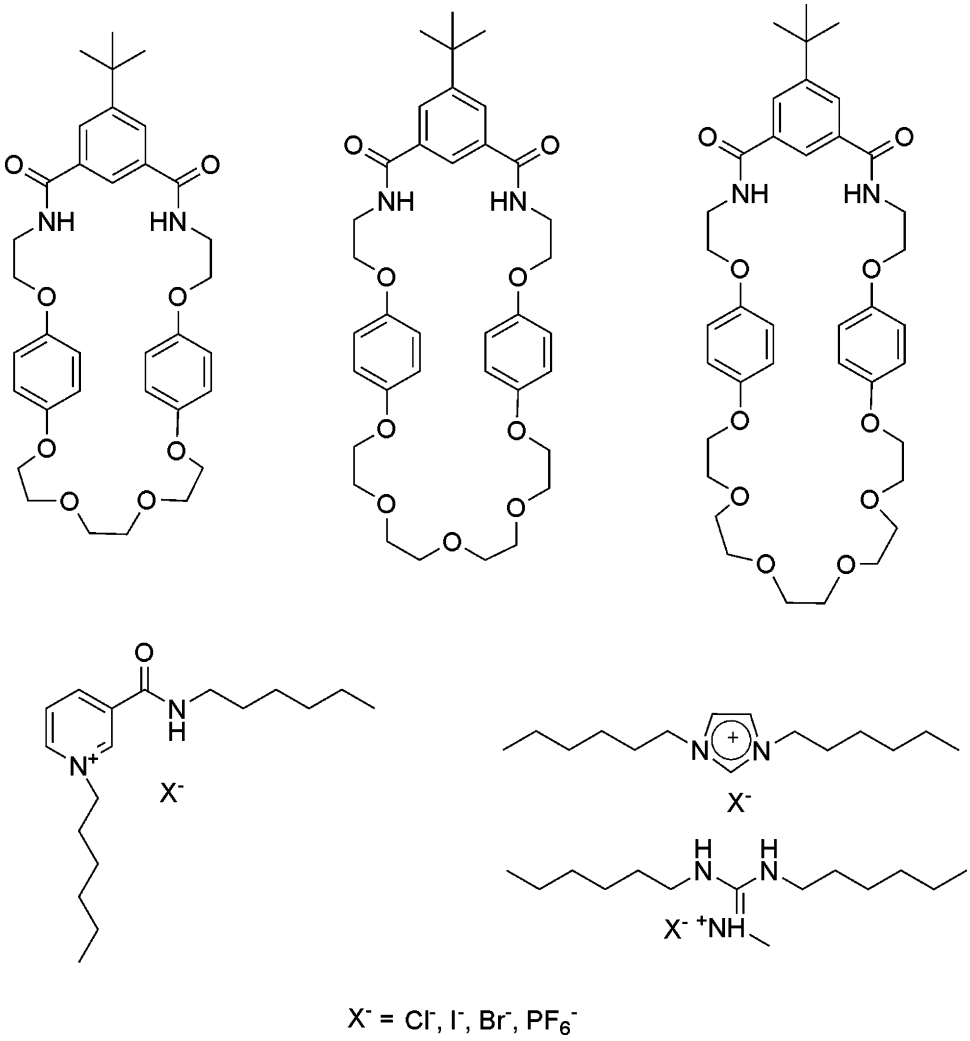

Scheme 8. Schematic representation of the macrocycles and linear cationic molecules used as "wheels" and "threads" for rotaxane formation.

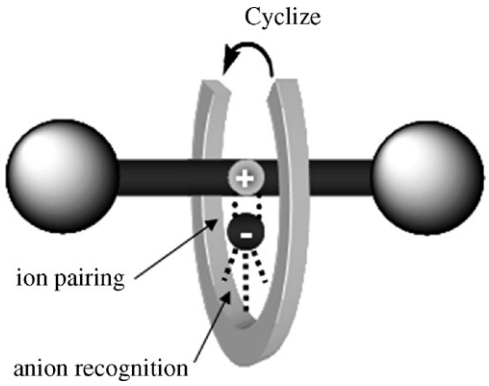

Fig. 25. Schematic representation of the anion-templated formation of a rotaxane by a clipping procedure.

shifts of the amide and the *ortho*-isophthalimide ring protons of the macrocycle ($\delta = 2.24$ and 0.70 ppm, respectively) indicated the complexation of the anion by this hydrogen-bonding cleft. The single crystal X-ray analysis of this species confirmed the formation of the interlocked product in which the macrocycle encircled the ion pair (see Fig. 26).

Once the anion-templated synthesis of the [2]rotaxane was achieved, the ability of this assembly to act as selective receptor for anions was studied. For this, the templating chloride from the initial [2]rotaxane was first replaced by the non-competitive anion $[PF_6]^-$. The binding of the [2]rotaxane towards acetate, dihydrogen phosphate and chloride was then investigated showing selectivity for chloride (with $K = 1300\,M^{-1}$ for Cl^-, $300\,M^{-1}$ for $[H_2PO_4]^-$ and $100\,M^{-1}$ for $[CH_3COO]^-$ in 1:1 $CDCl_3$:CD_3OD). These differences in anion selectivity could be ascribed to the formation of a unique hydrogen-bonding pocket by the diamide clefts of the cationic thread and macrocycle in the rotaxane, with a complementary topology for the chloride anion.

A further development of this methodology, involves the first examples of the anion-templated synthesis of [2] and [3]catenanes [61]. Compound **27** provided one macrocyclic unit of the target catenane (incorporating the amide cleft for anion recognition) while the pyridinium compound **28** was selected as thread to complement the binding sites of the macrocycle

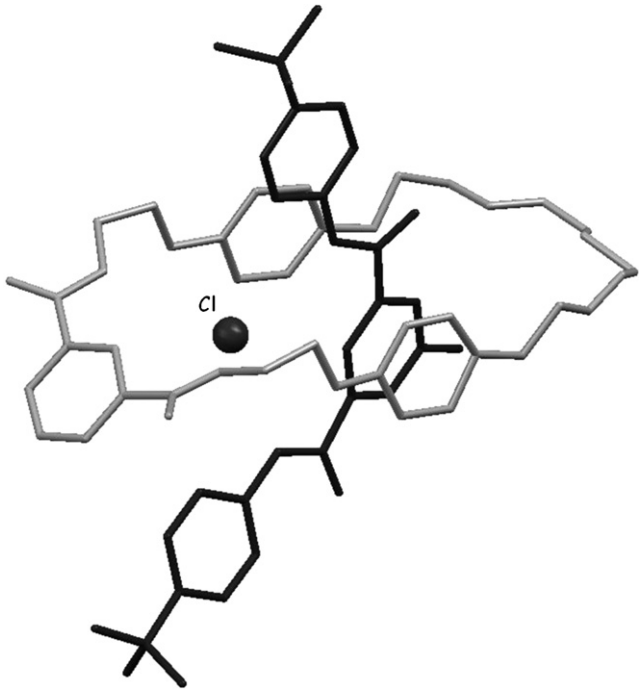

Fig. 26. Crystal structure of the rotaxane formed by a chloride-templated process from **25** and **26**. Cyclization of **25** was achieved by olefin metathesis using Grubbs' catalyst.

(see Scheme 10). Functionalization of the thread with terminal allylic groups enabled a ring closing metathesis reaction to be carried out yielding the [2]catenane (**29**) in 45% yield. Traces of a [3]catenane (<5%) were detected in this reaction. Single-crystal X-ray crystallography confirmed the interlocked nature of the two macrocyclic rings and the location of the chloride anion within the amide cavity (see Fig. 27).

The choice of anion in this process was shown to be crucial for the successful assembly of the interlocked species, chloride being the only one of the anions investigated to yield the [2]catenane in acceptable yield.

Using an analogous anion-templated approach to the one described above, a luminescent rotaxane has recently been reported by Beer and co-workers [62,63]. This assembly was prepared from the rhenium(I) bipyridyl derivative **30** (which

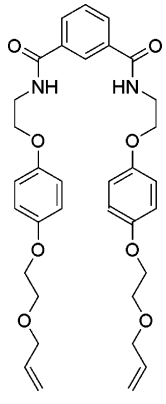

25

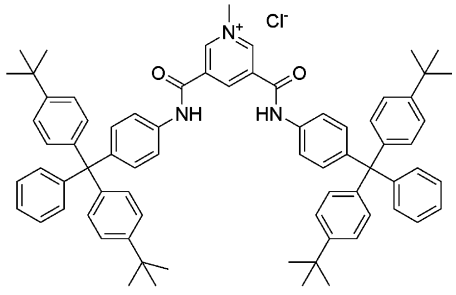

26

Scheme 9. Schematic representation of **25** and **26**.

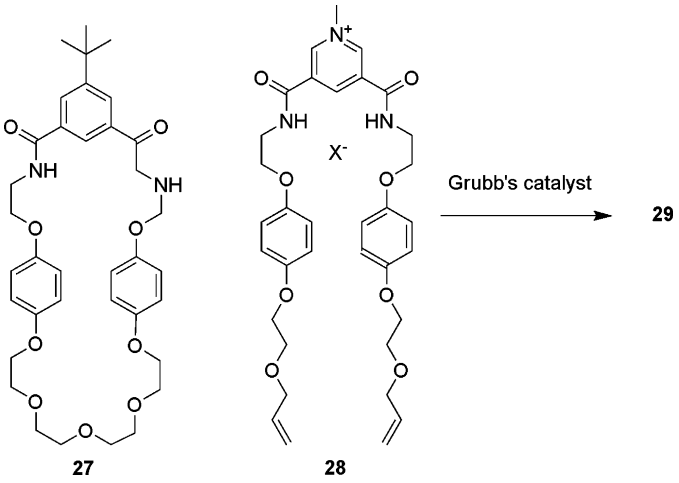

Scheme 10. Schematic representation of the anion-templated synthesis of catenane **29**.

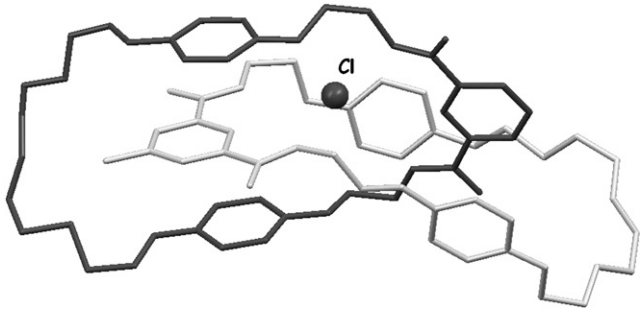

Fig. 27. Crystal structure of catenane **29** highlighting the position of the chloride.

is the precursor of the rotaxane's wheel) and the calix[4]arene pyridinium chloride axle **31**. In the presence of chloride, these two components were pre-organized so that when a ring closing metathesis was carried out with Grubb's catalyst the rotaxane **32** was obtained (see Scheme 11). Once **32** was formed and the templating chloride removed, anion binding studies were performed using the luminescence of the rhenium(I) moiety as the reporter signal. Addition of the tetrabutylammonium salts of chloride, nitrate and hydrogensulfate to acetone solutions of the rotaxane led to significant enhancement in emission intensity, in particular for the hydrogensulfate. Titration curves allowed to calculate anion association constants in acetone for the 1:1 complexes ($K > 10^6$ for $[HSO_4]^-$ versus $K = 1.81 \times 10^5$ for Cl^-). Interestingly, the selectivity of the rotaxane for the anions studied was opposite to that observed for the non-interlocked building blocks (namely **30** and the macrocycle resulting from ring closing metathesis of **30**). These systems showed to be more selective for chloride than hydrogensulfate ($K = 3.10 \times 10^5$ for Cl^- versus $K = 3.52 \times 10^3$ for $[HSO_4]^-$).

Stoddart and co-workers have recently described interlocked species where anions are not directly involved in their formation, but play a crucial role in determining the molecular motions of the components of these interlocked species [64,65]. One of these species is a rotaxane with an axle comprising two "stations": BPTTF and DNP [64]. The wheel of the rotaxane is positively charged and its motion from one station and the other can be induced electrochemically. Interestingly, depending of the counterion of the cationic ring one of the two translational isomers of the rotaxane is preferred over the other one (see Scheme 12).

In acetone, the PF_6^- rotaxane exits as an approximately 1:1 mixture of the two translational isomers where the cationic ring is located around the DNP recognition site in one isomer and around the BPTTF in the other. However, when the bulkier counterion TRISPHAT is used, the proportion of translational isomers changes in favor of the one with the cationic ring located in the BPTTF station (up to 95%). This preference towards the BPTTF station when having TRISPHAT could be explained as an electronic as well as a steric effect of a larger molecule, such as TRISPHAT.

3. Anion templates in the synthesis of polymeric materials

3.1. Coordination networks and polymers

Coordination networks have attracted great deal of interest over the past few years [66–69] due to their potential applications

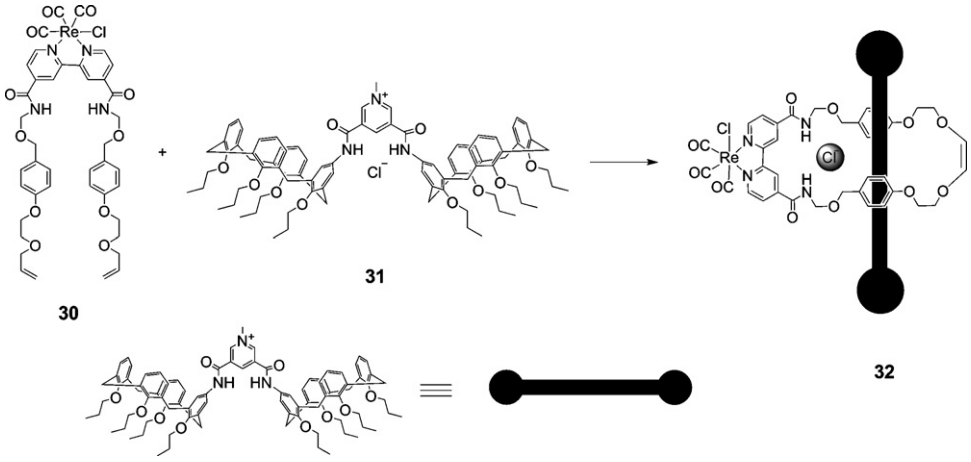

Scheme 11. Anion-tempalted synthesis of rotaxane **32**.

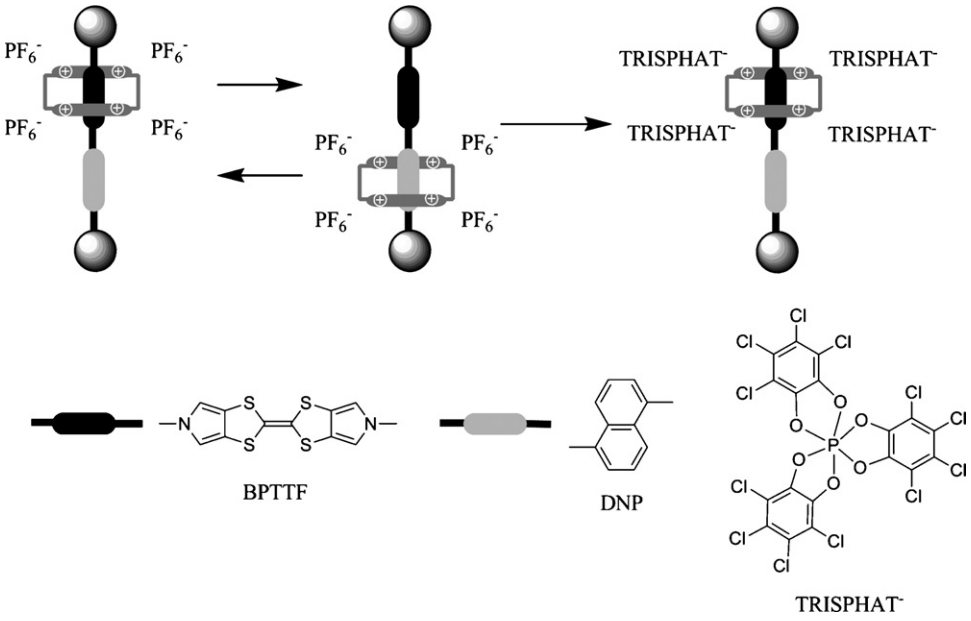

Scheme 12. Schematic representation of the translational isomerization induced by the presence of the TRISPHAT anion.

in sensing [70,71], storage [72–75] and catalysis [76,77]. For these applications to be realized, it is essential to have efficient synthetic procedures for their preparation. A common problem when synthesizing this type of assemblies is that, due to the dynamic nature of metal–ligand bonds and the various potential geometries that metal centers can take, it is often difficult to predict the exact nature of the final polymeric materials. The structures of metal-organic assemblies are highly dependent on the geometry, bulkiness and flexibility of the ligands employed as building blocks. The experimental conditions (such as the solvent, temperature and crystallization method) and the nature of the metals' counterions can also have an important influence on the structure of the final assembly.

Most of the metal-organic networks reported to date use metal cations with charges varying between +1 and +3. Since the metal assembly in the crystalline phase needs to have all the positive charges compensated by the corresponding negative charges, in the design of coordination networks it is possible to either use negatively charged ligands or have neutral ligands and use the metal's counter-anions to balance the charges. In the latter case, the counter-anions can be strongly coordinating and hence interact directly with the metal centre or be non-coordinating remaining as part of the network without interacting directly with the metal. However, in the latter case anions can still play a crucial role in determining the overall structure of the coordination network by acting as templates pre-organizing the ligands employed to build-up the assembly.

Due to this "dual" role of anions in coordination chemistry (i.e. negative ligands or non-coordinating counterions), it is usually difficult to separate the two phenomena when studying the influence that anions have in determining the final structure of a coordination network. Although in the past 5 years, there have been many reports on the formation of metal-organic frameworks using a wide range of ligands and metals, systematic studies on the influence of the anion in the final structure are not as common. In our previous review on anion templation [7], some of these studies were already presented showing the great influence that anions can have on the structures and properties of metal-organic materials formed. Following on from that discussion, a selection of more recent investigations in this area highlighting the dual coordinating/non-coordinating role of anions is herein presented.

We have recently studied the formation of a series of copper(II) coordination networks by reacting the hydrogen-bonding bipyridyl ligand **L^6** with different anions (see Scheme 13) [78].

As can be seen in Figs. 28–30, the structures obtained using $Cu(NO_3)_2$, $CuCl_2$, $Cu(OAc)_2$ and $CuSO_4$ as copper(II) sources are very different. At the time we started our investigations, the reaction between **L^6** and $Cu(NO_3)_2$ had been previously shown to yield a coordination network with formula $[Cu(\mathbf{L^6})_2(H_2O)(NO_3)][NO_3]$ [79], in which one of the nitrate anions is directly coordinated to the metal centre while the other one remains outside the coordination sphere interacting via hydrogen bonds with the urea groups of the ligand. We found a similar behaviour when the copper source

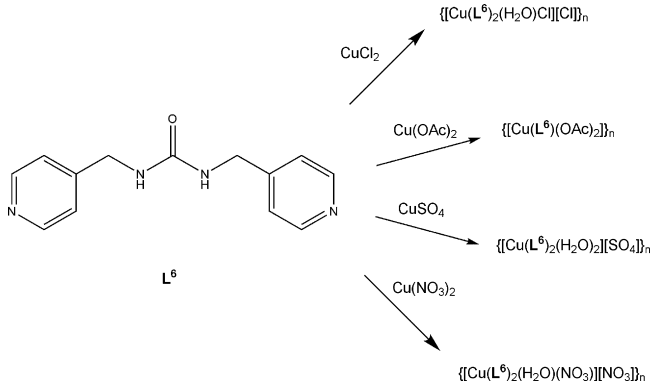

Scheme 13. Summary of the products resulting from the reactions between different copper(II) salts and **L^6**.

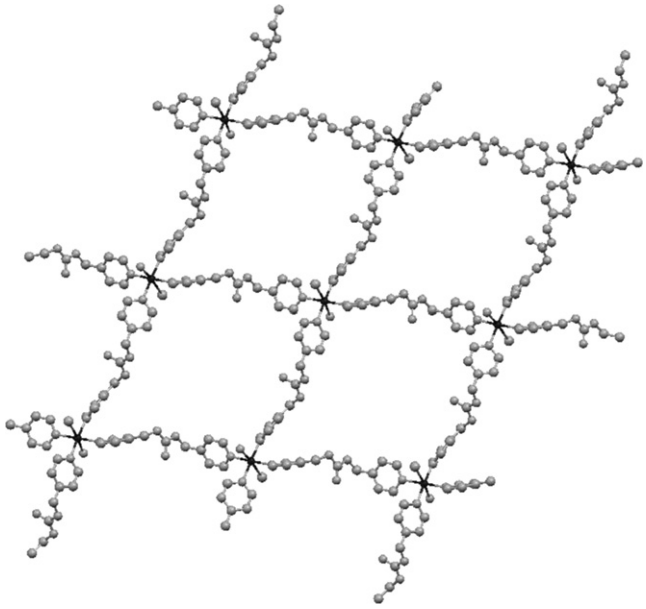

Fig. 28. Crystal structure of the infinite coordination network formed by $\{[Cu(\mathbf{L^6})_2(H_2O)Cl][Cl]\}_n$.

employed was $CuCl_2$: a non-interpenetrating grid of formula $\{[Cu(\mathbf{L^6})_2(H_2O)Cl][Cl]\}_n$ was formed with one of the chlorides directly bound to the metal centre while the second one remaining non-coordinated in the channels formed by the grids.

In contrast, when using $Cu(OAc)_2$, the assembly obtained consists of a 2D network of copper(II) centres coordinated in a square-based pyramidal fashion with three independent $\mathbf{L^6}$ molecules and two acetate ligands. In this assembly, with general formula $\{[Cu(\mathbf{L^6})(CH_3COO)_2]\}_n$, the equatorial positions of the copper centres are coordinated by two pyridine rings and two acetate anions while the axial position is occupied by a third ligand coordinated via its urea's carbonyl group (see Fig. 29). The coordination of each ligand $\mathbf{L^6}$ to three copper atoms via the pyridines and the oxygen of the urea group leads to the formation of a polymeric assembly of $Cu_2(\mathbf{L^6})_2$ rectangles.

Finally, the reaction between $CuSO_4$ and ligand $\mathbf{L^6}$, yielded yet a different assembly with formula $\{[Cu(\mathbf{L^6})_2(H_2O)_2][SO_4]\}_n$ (see Fig. 30). In this case, each copper(II) is coordinated to four independent ligands via their pyridyl groups and to two water molecules giving an octahedral geometry. In contrast to the other structures described above, the anions are not coordinated to the metals but are interacting via hydrogen bonds with the bridging bipyridyl ligand and the coordinated water molecules.

It is clear from the assemblies discussed above that anions have a very important influence – whether by direct coordination or non-coordinating counterions – in defining the final structure of metal-organic networks.

A large proportion of coordination networks and polymers are based on silver(I) or copper(I). Usually, these extended structures are prepared by mixing the corresponding metal salt with multipodal ligands in the appropriate stoichiometry. Since there are several potential ways in which the components can assemble together (due to the flexible coordination geometry around these metal centres) the "choice" of the final assembly is strongly influenced by the experimental conditions and by the nature of the metal's counter-anions. As discussed in our previous review, over the past few years several groups – such as those of Hannon [80], Min and Suh [81], Schröder [82], Keller [83,84] and Champness [85,86] – have carried out detailed investigations on the impact that anions have in the formation of metal-organic networks using silver(I) and copper(I).

Reger et al. have reported the formation of several silver(I) coordination networks and polymers using pyrazolyl-donor ligands, whose structures are highly dependant on several factors, one of them being the nature of the counter-anions [87,88].

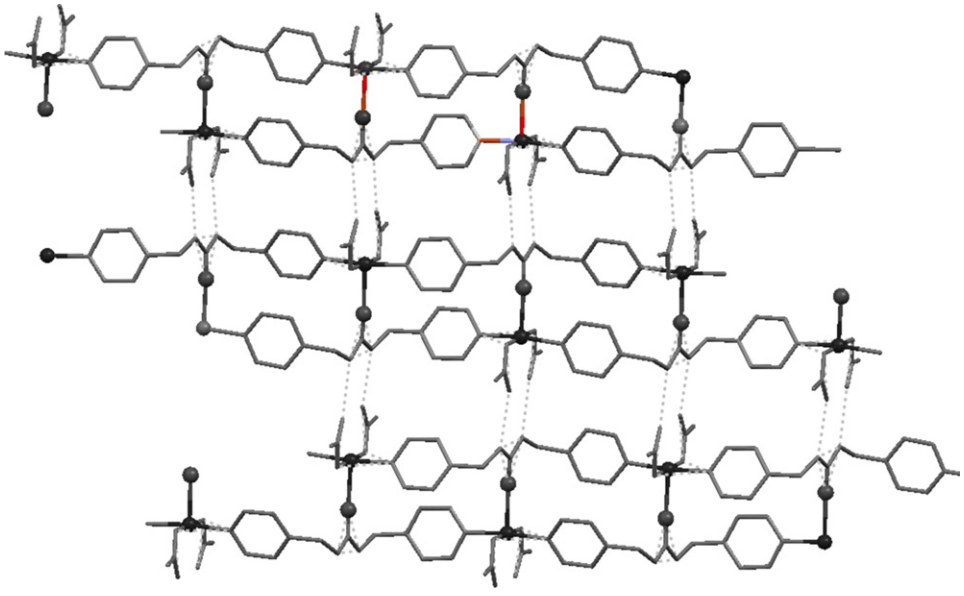

Fig. 29. Crystal structure of the polymeric chains of $\{[Cu(\mathbf{L^6})(CH_3COO)_2]\}_n$ highlighting the hydrogen-bonding interactions between the coordinated acetate groups and the N—H groups of the ligand's urea.

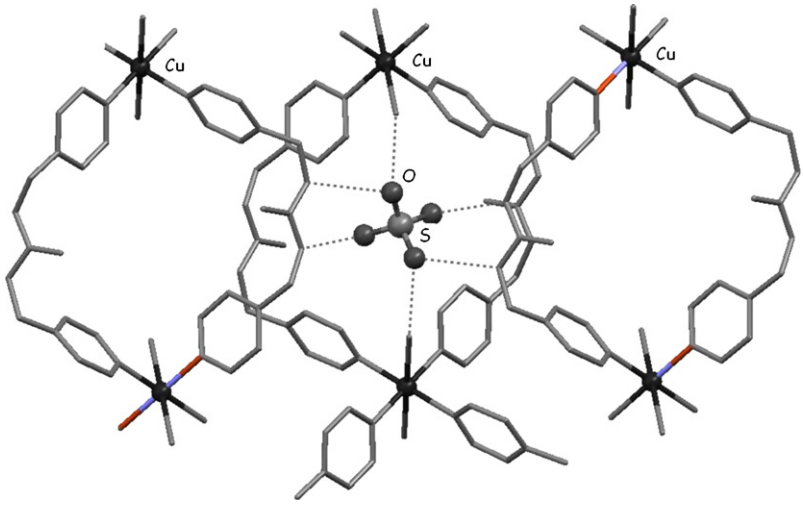

Fig. 30. A simplified view of the crystal structure of the polymeric assembly $\{[Cu(\mathbf{L^6})_2(H_2O)_2][SO_4]\}_n$ highlighting the hydrogen-bonding interactions of the encapsulated sulfate anion.

More specifically, this group has reported the assemblies resulting from the reactions between three different silver salts (namely AgX with X = BF_4, CF_3SO_3, NO_3) and the tetrapyrazole ligand 1,1,5,5-tetra(1-pyrazolyl)pentane $[CH(pz)_2(CH_2)_3CH(pz)_2$, $\mathbf{L^7}]$ (see Scheme 14) [88]. When $AgBF_4$ or $Ag(CF_3SO_3)$ were used discrete [2 + 2] macrocycles with formula $[Ag_2(\mathbf{L^7})_2][X]_2$ were obtained and structurally characterised (see Fig. 31).

In these assemblies, the anions are non-coordinating and positioned outside the cyclic structures. Interestingly, with $[BF_4]^-$ the anion does not display any important supramolecular interactions with the metalla-cycles and hence does not play a role in defining the extended supramolecular structure of the system in the solid state. On the other hand, the $[CF_3SO_3]^-$ anions are involved in multiple non-covalent interactions (including hydrogen-bonding) with the metalla-cycles leading to the formation of supramolecular chains in the solid state (see Fig. 32).

In contrast to the behaviour observed with the previous two anions, when $AgNO_3$ is employed in this reaction a coordination polymer with formula $\{[Ag(\mathbf{L^7})][NO_3]\}_n$ is obtained (see Fig. 33). In this assembly, each bis(pyrazolyl)-methane unit coordinates in a bidentate fashion. In addition, a weakly bonded bidentate nitrate completes a pseudo-octahedral environment around the silver(I) centres. The polymeric chains formed in this way, interact with each other via Ag–O and CH···O to generate a 3D supramolecular structure in the solid state.

In the same paper, the authors also investigate the influence that the length of the spacer that links the bis(pyrazolyl)-methane units has in the structure of the metalla-assemblies. The reactions between the same silver(I) salts discussed above and the shorter ligand $[CH(pz)_2(CH_2)_2CH(pz)_2]$ were investigated and the structures reported. Once again, the anions play an important role yielding discrete metalla-macrocycles for X = $[BF_4]^-$ or $[CF_3SO_3]^-$, and a coordination polymer (of metalla-cycles) for X = $[NO_3]^-$.

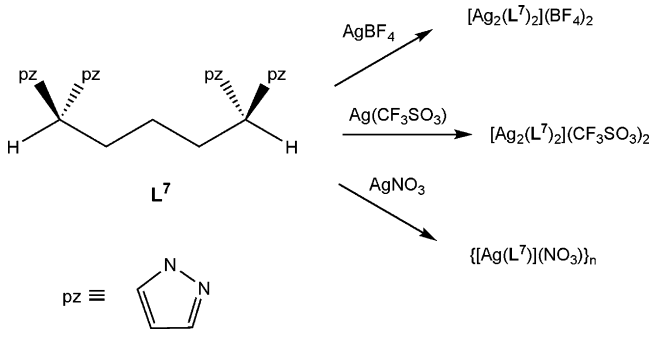

Scheme 14. Summary of the products resulting from the reactions between different silver(I) salts and $\mathbf{L^7}$.

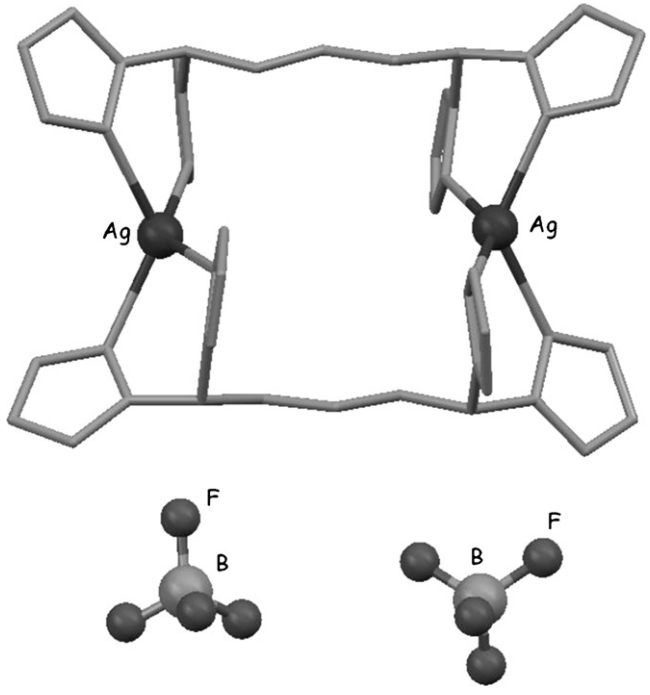

Fig. 31. Crystal structure of $[Ag_2(\mathbf{L^7})_2](BF_4)_2$ showing the anions outside the macrocyclic cavity.

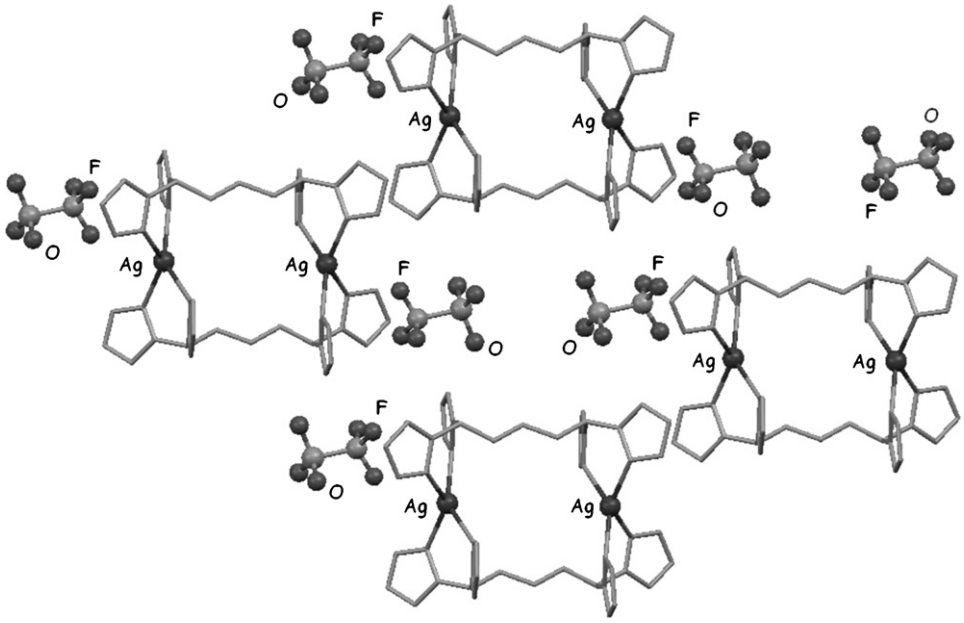

Fig. 32. Crystal structure of $[Ag_2(\mathbf{L}^7)_2](CF_3SO_3)_2$ showing the extended structure formed due to non-covalent interactions between the triflate anions and the metalla-macrcocyles.

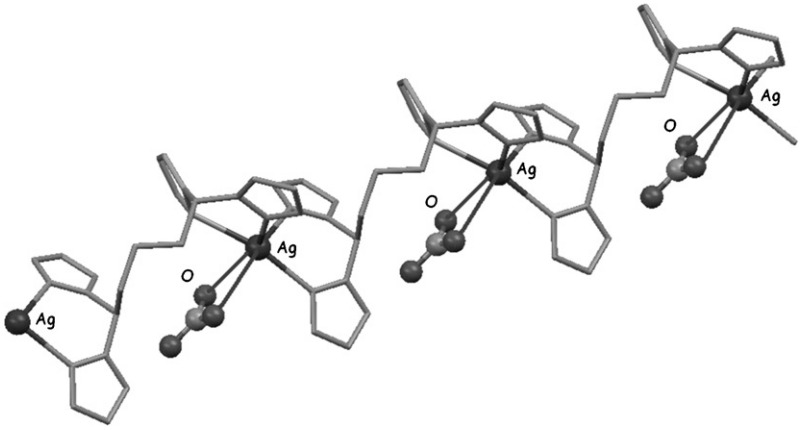

Fig. 33. Crystal structure of the coordination polymer $\{[Ag(\mathbf{L}^7)][NO_3]\}_n$ showing the coordination of the nitrate anions to the silver(I) centres.

Cheng and co-workers have recently reported a series of polymeric metalla-assemblies based on zinc(II) or cadmium(II) whose final structures depend greatly on the counter-anion present [89]. The reactions of MX_2 (where M = Zn or Cd; X = Cl, NO_3 or ClO_4) with the bridging ligand 1,2-bis(1,2,4-triazole-1-yl)ethane, $\mathbf{L}^8$ (see Scheme 15) were investigated and the crystal structures of some of the resulting assemblies reported.

When the reaction was carried out with $ZnCl_2$, a helical infinite chain with formula $[Zn(\mathbf{L}^8)Cl_2]_n$ was formed (see Fig. 34). The coordination around the zinc(II) centres in this coordination polymer is tetrahedral yielding a helix with a width of ca. 8.3 Å and a pitch of ca. 12.3 Å containing two zinc(II) ions per turn. Several non-covalent interactions – such as C–H···Cl hydrogen bonds – are observed in this structure which help stabilising the coordinated helical chains. Furthermore, the chains intertwine yielding double helical arrangements of these coordination polymers.

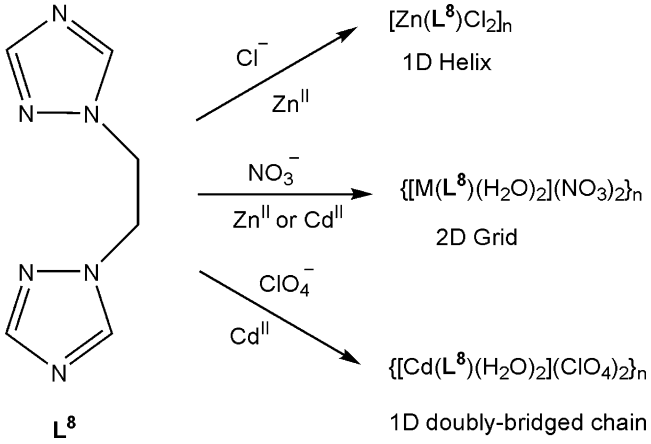

Scheme 15. Summary of the products resulting from the reactions between different zinc(II) and cadmium(II) salts and $\mathbf{L}^8$.

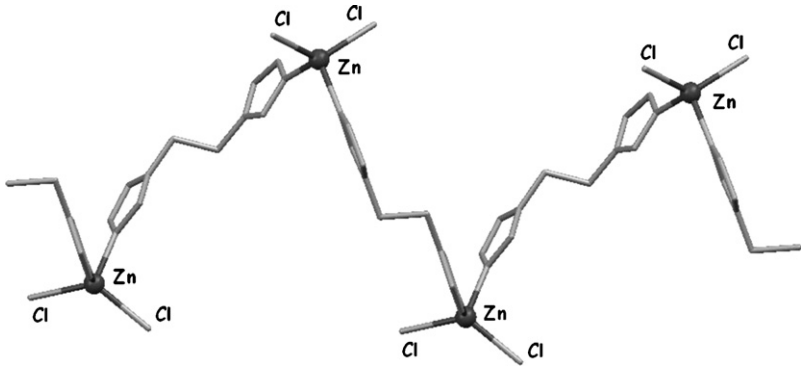

Fig. 34. Crystal structure of the right-handed helical infinite chain $[Zn(\mathbf{L^8})Cl_2]_n$.

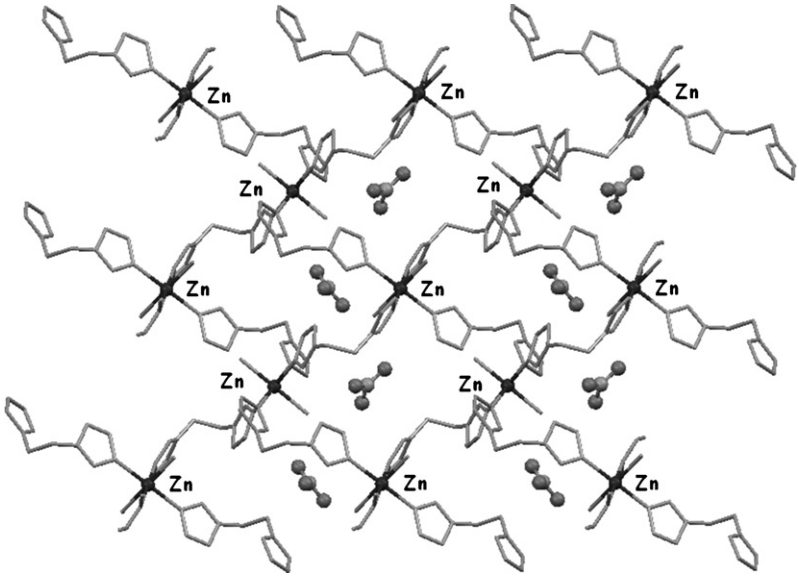

Fig. 35. Crystal structure of the two-dimensional coordination polymer $\{[Zn(\mathbf{L^8})_2(H_2O)_2](NO_3)_2\}_n$ showing the nitrate anions imbedded in the network.

In contrast, when either $Zn(NO_3)_2$ or $Cd(NO_3)_2$ are used as metal sources, two-dimensional coordination polymers with formula $\{[M(\mathbf{L^8})_2(H_2O)_2](NO_3)_2\}_n$ (M = Zn, Cd) are formed (see Fig. 35).

The metal centres have octahedral geometry with four ligands equatorially located and two axial water ligands. The nitrate counter-anions are imbedded in the network interacting via hydrogen bonds with the coordinated water molecules forming 1D supramolecular zigzag chains.

Finally, the reaction between $\mathbf{L^8}$ and $Cd(ClO_4)_2$ yields yet a different polymeric assembly, namely a 1D double-bridged assembly with formula $\{[Cd(\mathbf{L^8})_2(H_2O)_2](ClO_4)_2\}_n$ (see Fig. 36).

The metal centres have an octahedral coordination with four ligands in the equatorial plane and two water molecules in the axial positions. In contrast to the structure formed when using $M(NO_3)_2$, here two cadmium centres and two ligands form metalla-macrocycles which link with the neighbouring macrocycle to yield the structure shown in Fig. 36. The perchlorate counter-anions are involved in Cl···H–O hydrogen-bonding with the coordinated water molecules leading to the formation of a higher order supramolecular assembly.

An interesting study on the control exerted by anions in defining the secondary structure of a series of silver(I) coordination polymers has been recently reported by Lee and co-

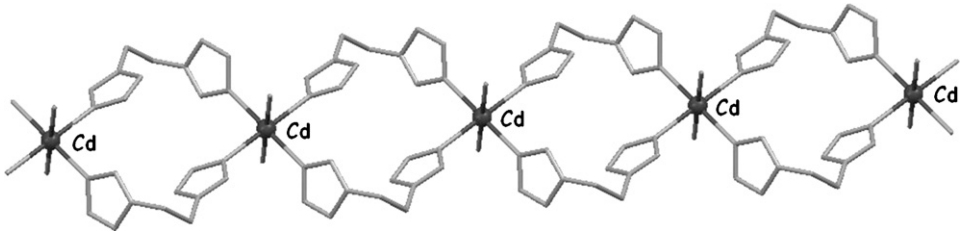

Fig. 36. Crystal structure of the 1D double-bridged polymeric assembly $\{[Cd(\mathbf{L^8})_2(H_2O)_2](ClO_4)_2\}_n$.

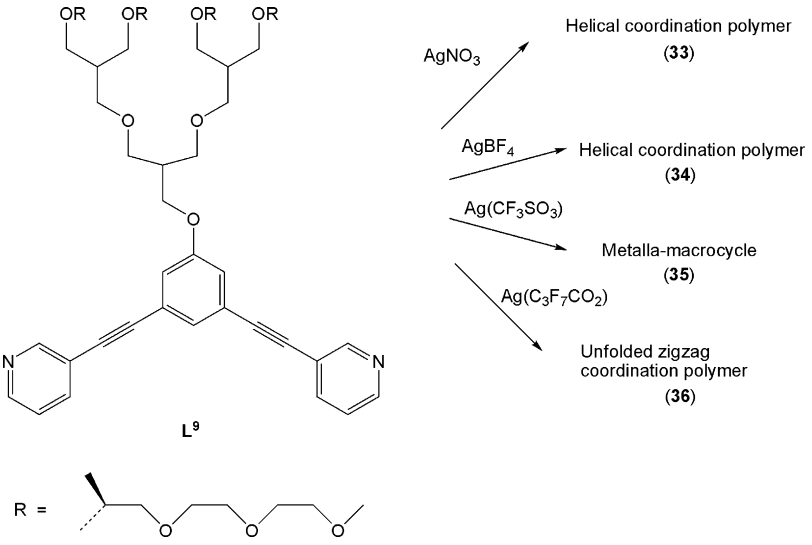

Scheme 16. Summary of the assemblies resulting from the reaction between different silver(I) salts and $\mathbf{L}^9$.

workers [90]. Using the bent-shaped bipyridyl ligand ($\mathbf{L}^9$) shown in Scheme 16, this group has shown – using 1D and 2D X-ray diffraction experiments – that as the size of the counter-anion increases the secondary structure of this assembly in the solid state changes from a folded helical chain to an unfolded zigzag conformation. As a consequence of this, the aggregation behaviour of the coordination chains changes dramatically in the presence of different anions.

The solid state structure of these assemblies was confirmed by small- and wide-angle X-ray measurements. These studies showed that for smaller anions, such as $[NO_3]^-$ and $[BF_4]^-$, the cationic coordination chains can bind effectively an anionic guest (through a *cisodial* conformation) yielding a helical arrangement that organizes into a 2D hexagonal columnar structure (see Fig. 37). While X-ray studies show that complex **34** exhibits an intramolecular order, complex **33** (with $[NO_3]^-$) has only a liquid-like order within the column. This is probably due to the fact that $[NO_3]^-$ is too small as a guest for the cavity formed by the helical assembly which hence contracts to bind the anion efficiently leading to a disorder of the helical pitch within the column.

In the case of the assembly formed with $Ag(CF_3SO_3)$, the X-ray studies in combination with simple CPK models suggest that the triflate counter-anion can be closely encapsulated by a metalla-cycle formed by two ligands and two silver(I) centres (**35**). These macrocyclic species are proposed to self-assemble into a tubular (helical) structure, which organizes into a two-dimensional lattice (see Fig. 38).

The authors rationalize this structure (in comparison to the helical chains formed with $[BF_4]^-$) by indicating that the size of the cavity in **35** is enlarged for effective binding of the larger triflate anion generating the macrocycles which self-assemble into tubular arrangements. Furthermore, the macrocycles stack with mutual rotation to avoid the steric hindrance generated by the bulky dendritic substituents of the ligand. This generates the helical columns observed in the secondary structure of this complex (see Fig. 38).

In contrast to the helical structures described above, in the presence of the bulkier heptafluorobutyrate anion, the silver(I) coordination chains (**36**) adopt unfolded zigzag conformation (see Fig. 39). This is most likely due to the larger size of the anion, which prevents it from being encapsulated by the silver–ligand system.

The X-ray diffraction experiments of **36** also indicate that the unfolded zigzag coordination chains self-assemble into a lamellar structure with in-plane two-dimensional order.

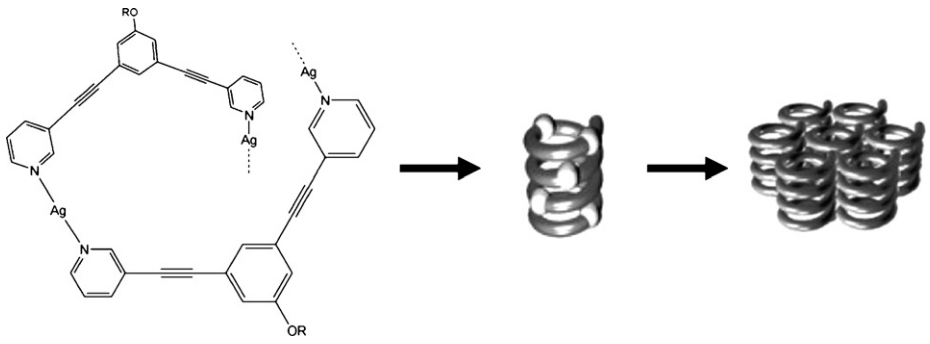

Fig. 37. Molecular formula of the polymeric helical arrangement of **34** and schematic representation of its secondary structure (figure taken from ref. [90]; *J. Am. Chem. Soc.* 126 (2004) 7009—reproduced by permission of The American Chemical Society).

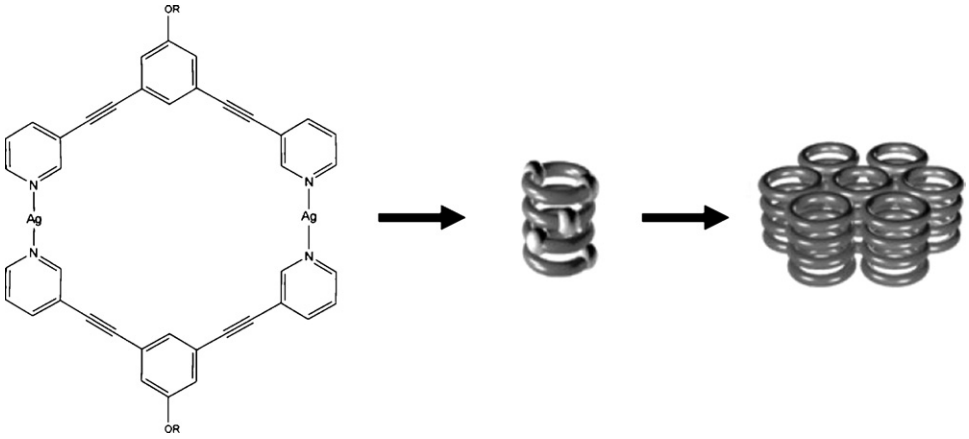

Fig. 38. Molecular formula of the metalla-macrocycles formed by **35** and schematic representation of its secondary structure (figure taken from ref. [90]; *J. Am. Chem. Soc.* 126 (2004) 7009—reproduced by permission of The American Chemical Society).

3.2. Molecularly imprinted polymers

Molecularly imprinted polymers (MIP) are materials capable of recognizing and binding specific substrates [91,92]. They are normally prepared by polymerizing functional monomers in the presence of a specific templating agent, which generates "cavities" complementary in size, shape and function to the original template. Consequently, these polymers are able to act as selective hosts for specific guests having potential applications as material for selective separation, sensing and catalysis (enzyme mimics).

Although MIPs have been studied for several years and imprinted materials for a wide range of substrates have been obtained, until recently there were only few examples reported of MIPs templated by anionic species. For example, the MIPs independently reported by Shinkai and co-workers [93] and Powell and co-workers [94] in the late 1990's demonstrated to be good polymeric hosts for AMP and cAMP.

Over the past 4 years, several new examples of anion-templated MIPs have been reported. Wulff, for example, has used phosphate and phosphonate templates to prepare imprinted polymers that mimic the active site of carboxypeptidase-A (a zinc-containing enzyme that hydrolyses peptide bonds) [95]. The functional monomer **37** (containing a benzamidine group as a hydrogen bond donor and a triamine to coordinate Zn^{II}) was polymerized by radical initiation together with ethylene dimethacrylate (EDMA), methylmethacrylate (MMA), the template (either diphenylphosphate (**38**) or phenyl-2-pyridylphosphate (**39**)) and $ZnCl_2$ (see Fig. 40).

After removal of the template, the catalytic ability of the imprinted polymers to hydrolyse diphenylcarbonate was studied and compared to a control polymer prepared under the same conditions but without the anionic template. The MIP prepared with **38** as a template, gave 1800-fold rate enhancement of the hydrolysis reaction in comparison to the control. The enhancement was even higher (3200-fold) for the MIP prepared using **39**

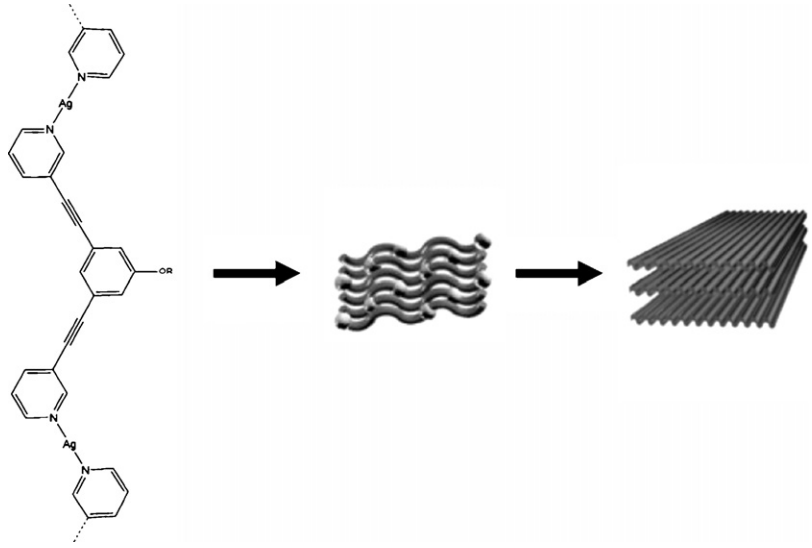

Fig. 39. Molecular formula of the unfolded coordination polymer formed by **36** and schematic representation of its secondary structure (figure taken from ref. [90]; *J. Am. Chem. Soc.* 126 (2004) 7009—reproduced by permission of The American Chemical Society).

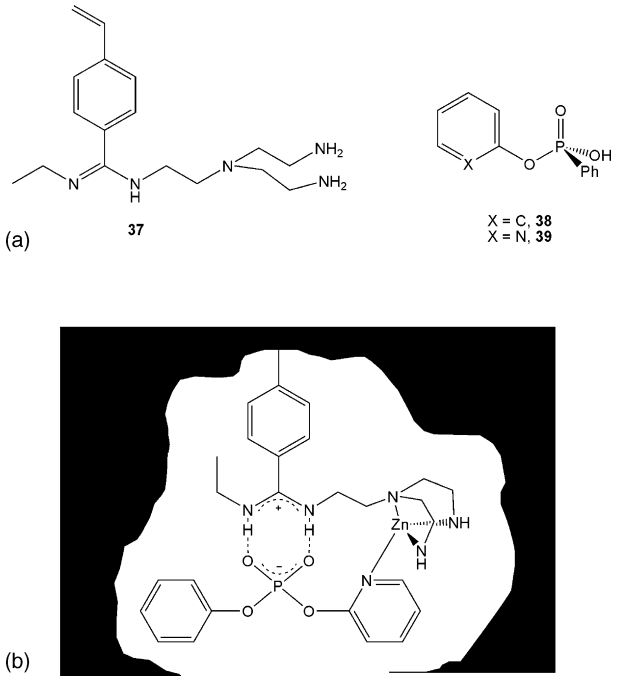

Fig. 40. (a) Molecular formula of the monomer and building blocks used to generate the MIP shown in (b).

as template. The high activity of the later can be explained by the complexation of the pyridine group of template **39** that stabilizes a favourable conformation during imprinting. In a similar study by the same authors, it was shown that Cu^{II} can also be used in the catalytic centre and also that a wider range of substrates can be hydrolysed [96].

In another recent development, Spivak has published a survey of several commercially available functional monomers to yield MIPs with selectivity to bind carboxylates and phosphonic acids [97]. Up to five aromatic and aliphatic functional commercial monomers containing binding moieties were explored (see Scheme 17). All of them were polymerized in the presence of the template *t*boc-L-phenylalanine, which contains a single chiral centre allowing enantioselectivity.

The different MIPs obtained were evaluated by HPLC and the retention factors were employed to calculate separation factors of L- and D-enantiomers of the *t*boc-Phe. These values allow comparison of binding and selectivity of the MIPs studied. The results showed a higher selectivity for the MIPs

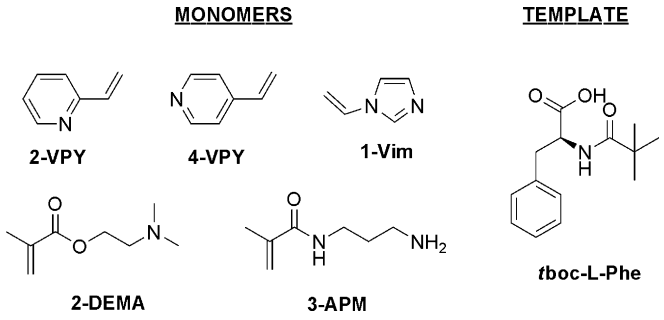

Scheme 17. Schematic representation of the different monomers and template for the synthesis of MIPs.

prepared using the pyridine-derivatives 2-VPY and 4-VPY than with the aliphatic amines. In contrast, the highest binding affinity – though poorer selectivity – was obtained for the MIPs prepared with the aliphatic amine monomers 2-DEMA and 3-APM. This effect was explained to be due to the more directional and specific interaction of the aromatic amines while the more charged and more basic aliphatic amines provide strongest binding interactions increasing the affinity of the MIPs for the guest.

Phosphate imprinted MIPs were prepared with 2-VPY and 2-DEMA to evaluate binding and selectivity for this anion. Chiral aminophosphonic acids were used in this study, which have, in general, much better affinity for MIPs than carboxylates. However, only the polymer containing the 2-VPY showed selectivity against the phosphate. Indeed, it seemed that the selectivity achieved with the phosphate was not as good as the one achieved with an analogous carboxylate. This was explained due to the reduced specificity of the interaction of both phosphate groups against a single interaction of the carboxylate. Moreover, specificity of 2-VPY containing polymer had an important dependence on the pH.

The development of MIPs for imprinting small and simple molecules, such as low molecular weight carboxylic acids, is often troublesome as good selectivities are not easily achieved. Li reported an indirect method to prepare 4-vynilpyridine MIPs using copper complexes of the corresponding carboxylic acids as templates [98]. Polymers imprinted with formic, acetic or propionic acid showed very low retention factors (0.028, 0.069 and 0.070, respectively). Both computational and chromatographic studies pointed out that this non-imprinting effect is probably due to the fact that these molecules are too small and simple and the cross-linking agent cannot form a regular cavity fitted for them. Enlarging the size of the template and strengthening the interaction between template and functional monomer by forming, in this case, picolinamide-copper complexes, such as the ones shown in Fig. 41, improve the selectivity of the MIPs towards the acid-complex (25.9, 9.2 and 18.65 for formic, acetic and propyonic acid, respectively) and indirectly to the acid itself.

3.3. Liquid crystals

An area of great current interest is the development of columnar and cubic thermotropic liquid crystals [99–101] from self-organization of anisometric molecules [102,103]. One of the approaches employed to build and manipulate these interesting materials is based on supramolecular interactions between a binding motif in the anisometric molecule and a complementary guest. This approach has the advantage of being very versatile and flexible since in the presence of different guests the same molecules could yield very different materials.

Although the systematic use of anionic guests to template the formation of specific liquid crystalline structures has not been widely studied, a recent report by Kim et al. demonstrates the important role that anionic guests can play in this area [104]. More specifically, this group has reported the effect of the size and nature of anions in the mesomorphic behaviour of a series of self-organized structures based on the wedge-shaped guanidinium derivative **40** (see Fig. 42). The guanidinium moiety is

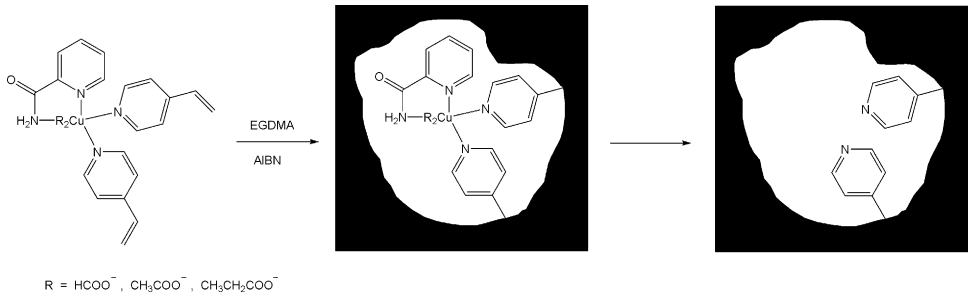

Fig. 41. Schematic representation of the formation of a MIP by using copper(II) complexes with carboxylate ligands as templates.

well-known to form strong host–guest complexes with several anions through electrostatic as well as hydrogen-bonding interactions.

Compound **40** yields several different self-organized structures depending of the counter-anion employed. For example, with the polyatomic anions $[NO_3]^-$ or $[BF_4]^-$, a hexagonal columnar mesophase was formed. Changing to a cylindrical anion, such as $[HCCCO_2]^-$, a rectangular columnar mesophase was obtained, indicating that the anion has an effect not only in the formation of columnar phases but also in the selection of a preferred arrangement of such columns. Finally, Cl^- (a smaller and spherical anion) favors the formation of both a columnar mesophase and a cubic phase, which are not very common phases in liquid crystals.

The authors propose that the different arrangements of [**40**]X are due to the formation of a supramolecular structure where four molecules of **40** assemble with the corresponding anion to yield a disk-type assembly (see Fig. 42). These disks stack on top of each other yielding an infinite column "glued" together via favorable intermolecular non-covalent interactions. The spherical (Cl^-) and highly symmetrical ($[NO_3]^-$ or $[BF_4]^-$) anions favor hexagonal arrangements. On the other hand, the less symmetrical and linear $[HCCCO_2]^-$ anion yields a rectangular arrangement. A further interesting observation with the chloride-containing system is that, when increasing the temperature, an inverted micellar cubic phase is formed. This could be explained as a collapse of the cylinders at higher temperatures resulting in formation of spherical aggregates, which are only favoured in the case of a small and spherical anion, such as Cl^-, with no preferred binding directionality.

4. Anions as templates in dynamic combinatorial libraries

The pioneering work by Sanders [105–108] and Lehn [109–111] on dynamic combinatorial chemistry has become a powerful approach for the synthesis of selective molecular receptors [112]. This approach is based on the generation of a dynamic combinatorial library (DCL) of compounds formed by linking different building blocks using reversible covalent or non-covalent reactions. The use of a reversible reaction allows the different members of the library to interconvert continuously, generating a mixture of compounds in equilibrium. Because of the dynamic equilibria established in a DCL, the stabilization of any given compound by molecular recognition can amplify its formation. Hence, the addition of a template to the library under the right experimental conditions, generally leads to the isolation of the compound that forms the thermodynamically more stable host–guest complex with the added template.

These virtual libraries may be applied either to aid the discovery of a substrate for a particular receptor (defined by Lehn as casting) or for the construction of a particular receptor for a given guest (defined by Lehn as molding). Both these approaches to DCLs rely not only on the reversible formation of bonds between the different basic components of the mixture, but also on their ability to display interactions (e.g. non-covalent, such as hydrogen bonds) with the template.

A critical step in the generation of a DCL is the selection of the adequate reaction to generate the library of potential receptors. Different covalent reversible reactions, such as hydrazone formation, disulfide exchange or imine formation are commonly

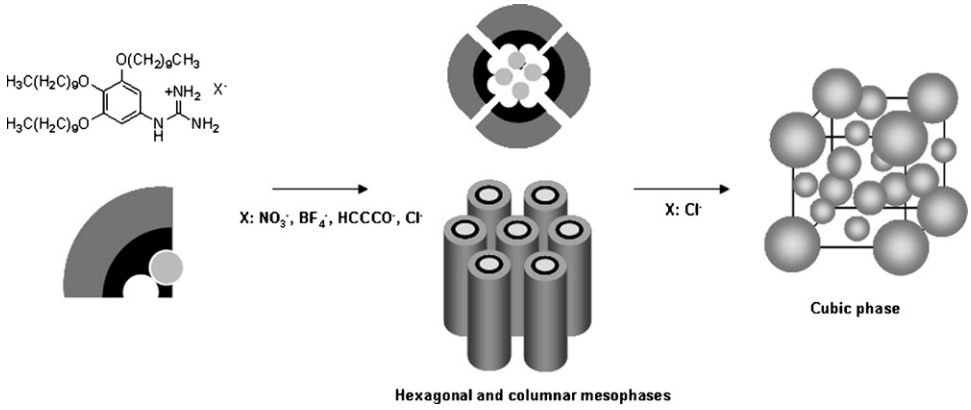

Fig. 42. Schematic representation of the different self-assembled liquid crystalline materials obtained in the presence of different anions.

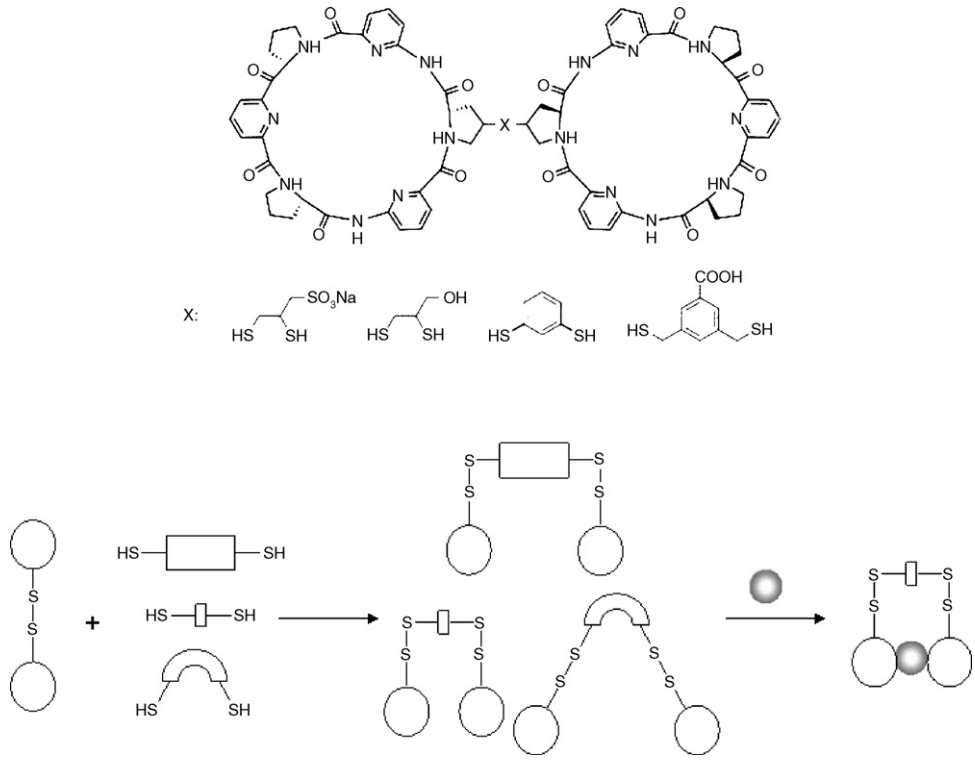

Fig. 43. Schematic representation of a dynamic combinatorial library of anionic receptors based on cyclic peptides and dithiols.

employed to generate the DCL. Since non-covalent interactions, such as hydrogen-bonding are reversible, they can also be employed to generate these libraries.

Although in the past 10 years, there have been important advances in the area and dynamic combinatorial chemistry has been successfully applied to develop receptors for various cationic and neutral species, there are still very few examples of DCL's for anions. One of these examples has been recently published by Kubik and Otto who developed a dynamic library based on disulfide exchange to prepare neutral receptors for anionic species [113]. These receptors are based on dimers of cyclic peptides that are joined together by different thiol-containing spacers (see Fig. 43). The selectivity and binding properties of the dimers is highly dependant on the length and flexibility of these spacers.

For example, the addition of sulfate or iodide to a virtual library of these dimers (having different spacers as the structural variation) amplified the formation of one specific receptor. Addition of other anions, such as chloride or fluoride did not shift the equilibrium at all. Interestingly, isothermal titration calorimetry (ITC) studies revealed that the binding constants of the new dimeric-receptors with sulfate and iodide (with values around 10^6) are one order of magnitude higher than those for the monomeric cyclic peptides.

A different approach to the generation of dynamic libraries of anion-receptors has been proposed by Williams who has shown that chloride is capable of modifying the distribution of products in an equilibrated solution containing cobalt(II) and two different chelating ligands [114]. More specifically a mixture of 2,2′-bipyridyl, ligand $\mathbf{L^{10}}$ (see Scheme 18) and $Co(NO_3)_2$ generates a library of complexes with general formula $[Co(bipy)_X(\mathbf{L^{10}})_{3-X}]^{2+}$.

Since the octahedral coordination of chiral *N*,*N*′ chelating ligands to a metal centre can yield two different diastereoisomers (either Δ or Λ) several different complexes are expected to form. This was indeed the case when the mixture was analysed spectroscopically. Electrospray mass spectrometry showed that all the possible combinations of products were indeed present in solution in the following ratio: $[Co(\mathbf{L^{10}})_3]^{2+}$ (80%), $[Co(bipy)(\mathbf{L^{10}})_2]^{2+}$ (100%), $[Co(bipy)_2(\mathbf{L^{10}})]^{2+}$ (91%) and $[Co(bipy)_3]^{2+}$ (11%). Furthermore, ^{1}H NMR spectroscopy indicated that for each of the complexes – except for $[Co(bipy)_3]^{2+}$ which give an enantiomeric pair – the corresponding Δ- and Λ-diastereomers were present.

The equilibrium of the above mixture was shown to change when an acid (namely CF_3COOH) was added. This is due to the fact that protonation of the amines on $\mathbf{L^{10}}$ induce diastereoselectivity. In this way, some of the products initially present in

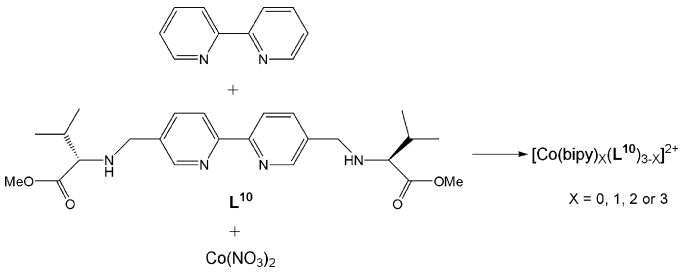

Scheme 18. Schematic representation of the products resulting from the reaction between cobalt(II), $\mathbf{L}^{10}$ and 2,2′-bipyridyl.

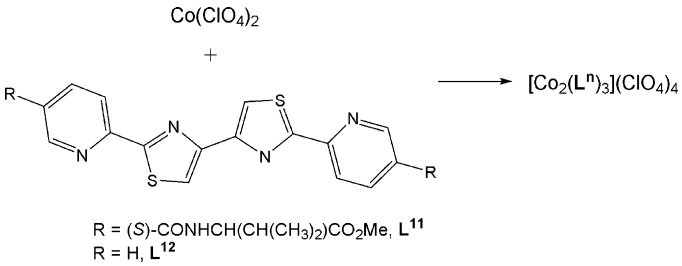

Scheme 19. Schematic representation of the reaction of a cobalt(II) salt and $\mathbf{L}^{11}$.

the mixture disappeared upon addition of the acid. Interestingly, an even more dramatic change in the distribution of products was observed when DCl instead of CF_3COOH was added to the dynamic library of complexes. The mixture shows essentially only two species, which the authors have identified on the basis of their ^{1}H NMR spectra as the homoleptic complexes $\{Cl_2\subset\Delta$-$[Co(\mathbf{L^{10}H_2})_3]^{6+}\}$ and $[Co(bipy)_3]^{2+}$. Although the host:guest complex amplified in this library is not particularly stable (as determined by binding constants), the authors rationalise the amplification of this complex on the grounds that coulombic repulsion between the protonated amines is minimized by the presence of chloride.

In a related system, Rice and co-workers have reported that nitrate can modify the distribution of products in a mixture of cobalt(II) and two different *N*,*N*′ chelating ligands [115]. In the investigation, the authors first showed that reacting $Co(ClO_4)_2$ with ligand $\mathbf{L}^{11}$ yields a triple helicate with formula $[Co_2(\mathbf{L}^{11})_3][ClO_4]_4$ (see Scheme 19).

In this metal complex, pockets for anion binding are formed at both ends of the helicate in each of which a perchlorate is bound via hydrogen bonds (see Fig. 44).

Interestingly, addition of two equivalents of $[Bu_4N][NO_3]$ to this complex yields the mixed-anion helicate $[Co_2(\mathbf{L}^{11})_3](ClO_4)_2(NO_3)_2$. The X-ray crystal structure of this complex shows that the perchlorates initially bound to the two anion-biding pockets of the helicate, have been replaced by nitrates.

Having established this, the authors investigated the distribution of products that would form upon mixing $[Co(ClO_4)_2]\cdot 6H_2O$, $\mathbf{L}^{11}$ and $\mathbf{L}^{12}$ (see Scheme 19 for the chemical structure of the ligands) in a 2:1.5:1.5 ratio. The ^{1}H NMR spectrum of this mixture indicated that the four complexes $[Co_2(\mathbf{L}^{11})_3]^{4+}$, $[Co_2(\mathbf{L}^{11})_2(\mathbf{L}^{12})]^{4+}$, $[Co_2(\mathbf{L}^{11})(\mathbf{L}^{12})_2]^{4+}$ and $[Co_2(\mathbf{L}^{12})_3]^{4+}$ in a statistical distribution of 1:3:3:1. This was confirmed by ES mass spectrometry, which also showed the presence of the four different complexes. However, when KNO_3 was added to this mixture the distribution of products changed dramatically with the two homoleptic complexes $[Co_2(\mathbf{L}^{11})_3]^{4+}$ and $[Co_2(\mathbf{L}^{12})_3]^{4+}$ being the main components of the mixture (with only 5% of the heteroleptic compounds). The authors attribute this behaviour to the strong binding of nitrate (which acts as a template) to the anion-binding pockets in $[Co_2(\mathbf{L}^{11})_3]^{4+}$.

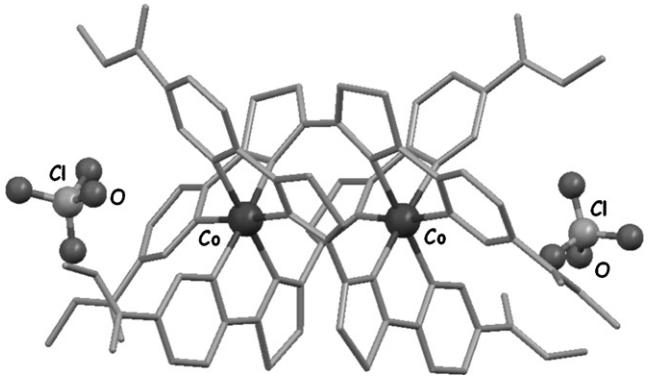

Fig. 44. Crystal structure of $[Co_2(\mathbf{L}^{11})_3][ClO_4]_4$ showing two of the perchlorate anions biding to the cavities generated by the helical arrangement of the ligands around the metal centres.

5. Conclusion

Not many years have passed since the first examples of anion-templated syntheses were reported in the early 1990's. However, over the past 5 years there have been an increasing number of processes in which anions play an important directing role. As has been shown in this review – which mainly covers the literature of the past 3 years – a wide range of molecular and supramolecular assemblies have now been prepared using anion-directed processes. This includes metal-containing cages and macrocycles, interlocked species (such as catenanes and rotaxanes) and helicates. Polymeric materials, both organic and metal-organic, with defined cavities have also been synthesized using this approach. Furthermore, anions have been used to modify the type of structures obtained in liquid crystalline materials leading to a potentially very useful approach to the control and manipulation of these materials. More recently, the first examples of dynamic combinatorial libraries of anionic receptors (using anions as templates) have appeared in the literature. This promises to be an efficient methodology for the preparation of selective receptors for anionic species.

Acknowledgements

We are grateful to the EU for financial support (grant NMP3-CT-2005-516982, HETEROMOLMAT).

References

[1] D.H. Busch, J. Inclusion Phenom. Mol. Recognit. Chem. 12 (1992) 389.
[2] F. Diederich, P.J. Stang (Eds.), Templated Organic Synthesis, Wiley-VCH, Weinheim, 2000.
[3] S. Anderson, H.L. Anderson, J.K.M. Sanders, Acc. Chem. Res. 26 (1993) 469.
[4] P.D. Beer, P.A. Gale, Angew. Chem. Int. Ed. 40 (2001) 486.
[5] A. Bianchi, K. Bowman-James, E. Garcia-Espana (Eds.), Supramolecular Chemistry of Anions, Wiley-VCH, New York, 1997.
[6] P.A. Gale, Coord. Chem. Rev. 240 (2003) 191.
[7] R. Vilar, Angew. Chem. Int. Ed. 42 (2003) 1460.
[8] C.S. Campos-Fernandez, B.L. Schottel, H.T. Chifotides, J.K. Bera, J. Bacsa, J.M. Koomen, D.H. Russell, K.R. Dunbar, J. Am. Chem. Soc. 127 (2005) 12909.
[9] C.S. Campos-Fernandez, R. Clerac, J.M. Koomen, D.H. Russell, K.R. Dunbar, J. Am. Chem. Soc. 123 (2001) 773.
[10] C.S. Campos-Fernandez, R. Clerac, K.R. Dunbar, Angew. Chem. Int. Ed. 38 (1999) 3477.
[11] J.T. Davis, Angew. Chem. Int. Ed. 43 (2004) 668.
[12] M. Roitzsch, B. Lippert, Angew. Chem. Int. Ed. 45 (2005) 147.

[13] R. Lin, J.H.K. Yip, K. Zhang, L.L. Koh, K.-Y. Wong, K.P. Ho, J. Am. Chem. Soc. 126 (2004) 15852.
[14] J.H.K. Yip, J. Prabhavathy, Angew. Chem. Int. Ed. 40 (2001) 2159.
[15] L. Raehm, L. Mimassi, C. Guyard-Duhayon, H. Amouri, M.N. Rager, Inorg. Chem. 42 (2003) 5654.
[16] M. Du, X.-H. Bu, Z. Huang, S.-T. Chen, Y.-M. Guo, C. Diaz, J. Ribas, Inorg. Chem. 42 (2003) 552.
[17] A. Bashall, A.D. Bond, E.L. Doyle, F. Garcia, S. Kidd, G.T. Lawson, M.C. Parry, M. McPartlin, A.D. Woods, D.S. Wright, Chem. Eur. J. 8 (2002) 3377.
[18] F. Garcia, J.M. Goodman, R.A. Kowenicki, I. Kuzu, M. McPartlin, M.A. Silva, L. Riera, A.D. Woods, D.S. Wright, Chem. Eur. J. 10 (2004) 6066.
[19] S. Ramos, E. Alcalde, G. Doddi, P. Mencarelli, L. Perez-Garcia, J. Org. Chem. 67 (2002) 8463.
[20] E. Alcalde, S. Ramos, L. Perez-Garcia, Org. Lett. 1 (1999) 1035.
[21] J.L. Sessler, M. Cyr, H. Furuta, V. Kral, T. Mody, T. Morishima, M. Shionoya, S. Weghorn, Pure Appl. Chem. 65 (1993) 393.
[22] E.A. Katayev, G.D. Pantos, M.D. Reshetova, V.N. Khrustalev, V.M. Lynch, Y.A. Ustynyuk, J.L. Sessler, Angew. Chem. Int. Ed. 44 (2005) 7386.
[23] R. Vilar, D.M.P. Mingos, A.J.P. White, D.J. Williams, Angew. Chem. Int. Ed. 37 (1998) 1258.
[24] R. Vilar, D.M.P. Mingos, A.J.P. White, D.J. Williams, Chem. Commun. (1999) 229.
[25] S.-T. Cheng, E. Doxiadi, R. Vilar, A.J.P. White, D.J. Williams, J. Chem. Soc. Dalton Trans. (2001) 2239.
[26] E. Doxiadi, R. Vilar, A.J.P. White, D.J. Williams, Polyhedron 22 (2003) 2991.
[27] P. Diaz, D.M.P. Mingos, R. Vilar, A.J.P. White, D.J. Williams, Inorg. Chem. 43 (2004) 7597.
[28] J.S. Fleming, K.L.V. Mann, C.-A. Carraz, E. Psillakis, J.C. Jeffery, J.A. McCleverty, M.D. Ward, Angew. Chem. Int. Ed. 37 (1998) 1279.
[29] R.L. Paul, Z.R. Bell, J.C. Jeffery, J.A. McCleverty, M.D. Ward, Proc. Natl. Acad. Sci. U.S.A. 99 (2002) 4883.
[30] R.L. Paul, S.P. Argent, J.C. Jeffery, L.P. Harding, J.M. Lynam, M.D. Ward, Dalton Trans. (2004) 3453.
[31] H. Amouri, L. Mimassi, M.N. Rager, B.E. Mann, C. Guyard-Duhayon, L. Raehm, Angew. Chem. Int. Ed. 44 (2005) 4543.
[32] A. Müller, H. Reuter, S. Dillinger, Angew. Chem. Int. Ed. Engl. 34 (1995) 2328.
[33] A. Müller, L. Toma, H. Boegge, M. Schmidtmann, P. Koegerler, Chem. Commun. (2003) 2000.
[34] M. Murugesu, R. Clerac, C.E. Anson, A.K. Powell, Chem. Commun. (2004) 1598.
[35] M. Murugesu, R. Clerac, C.E. Anson, A.K. Powell, Inorg. Chem. 43 (2004) 7269.
[36] X. Xu, E.J. MacLean, S.J. Teat, M. Nieuwenhuyzen, M. Chambers, S.L. James, Chem. Commun. (2002) 78.
[37] S.L. James, D.M.P. Mingos, A.J.P. White, D.J. Williams, Chem. Commun. (1998) 2323.
[38] P.D. Custer, J.C. Garrison, C.A. Tessier, W.J. Youngs, J. Am. Chem. Soc. 127 (2005) 5738.
[39] J. Sanchez-Quesada, C. Seel, P. Prados, J. de Mendoza, I. Dalcol, E. Giralt, J. Am. Chem. Soc. 118 (1996) 277.
[40] J. Keegan, P.E. Kruger, M. Nieuwenhuyzen, J. O'Brien, N. Martin, Chem. Commun. (2001) 2192.
[41] S.J. Coles, J.G. Frey, P.A. Gale, M.B. Hursthouse, M.E. Light, K. Navakhun, G.L. Thomas, Chem. Commun. (2003) 568.
[42] S.A. Nepogodiev, J.F. Stoddart, Chem. Rev. 98 (1998) 1959.
[43] M. Fujita, M. Tominaga, A. Hori, B. Therrien, Acc. Chem. Res. 38 (2005) 369.
[44] J.S. Siegel, Science 304 (2004) 1256.
[45] J.-C. Chambron, J.-P. Collin, V. Heitz, D. Jouvenot, J.-M. Kern, P. Mobian, D. Pomeranc, J.-P. Sauvage, Eur. J. Org. Chem. (2004) 1627.
[46] L. Raehm, J.-P. Sauvage, Struct. Bond. 99 (2001) 55.
[47] C. Reuter, R. Schmieder, F. Vogtle, Pure Appl. Chem. 72 (2000) 2233.
[48] V. Balzani, A. Credi, F.M. Raymo, J.F. Stoddart, Angew. Chem. Int. Ed. 39 (2000) 3348.
[49] T.J. Hubin, D.H. Busch, Coord. Chem. Rev. 200–202 (2000) 5.
[50] J.P. Sauvage, C. Dietrich-Buchecker (Eds.), Molecular Catenanes, Rotaxanes and Knots: A Journey Through the World of Molecular Topology, Wiley-VCH, Weinheim, 1999.
[51] F.M. Raymo, J.F. Stoddart, Chem. Rev. 99 (1999) 1643.
[52] R. Vilar, Struct. Bond. 111 (2004) 85.
[53] M.C.T. Fyfe, P.T. Glink, S. Menzer, J.F. Stoddart, A.J.P. White, D.J. Williams, Angew. Chem. Int. Ed. Engl. 36 (1997) 2068.
[54] P.R. Ashton, S.J. Cantrill, J.A. Preece, J.F. Stoddart, Z.-H. Wang, A.J.P. White, D.J. Williams, Org. Lett. 1 (1999) 1917.
[55] G.M. Hubner, J. Glaser, C. Seel, F. Vogtle, Angew. Chem. Int. Ed. 38 (1999) 383.
[56] C. Reuter, W. Wienand, G.M. Hubner, C. Seel, F. Vogtle, Chem. Eur. J. 5 (1999) 2692.
[57] J.A. Wisner, P.D. Beer, M.G.B. Drew, Angew. Chem. Int. Ed. 40 (2001) 3606.
[58] J.A. Wisner, P.D. Beer, N.G. Berry, B. Tomapatanaget, Proc. Natl. Acad. Sci. U.S.A. 99 (2002) 4983.
[59] M.R. Sambrook, P.D. Beer, J.A. Wisner, R.L. Paul, A.R. Cowley, F. Szemes, M.G.B. Drew, J. Am. Chem. Soc. 127 (2005) 2292.
[60] J.A. Wisner, P.D. Beer, M.G.B. Drew, M.R. Sambrook, J. Am. Chem. Soc. 124 (2002) 12469.
[61] M.R. Sambrook, P.D. Beer, J.A. Wisner, R.L. Paul, A.R. Cowley, J. Am. Chem. Soc. 126 (2004) 15364.
[62] D. Curiel, P.D. Beer, R.L. Paul, A. Cowley, M.R. Sambrook, F. Szemes, Chem. Commun. (2004) 1162.
[63] D. Curiel, P.D. Beer, Chem. Commun. (2005) 1909.
[64] W. Laursen Bo, S. Nygaard, O. Jeppesen Jan, J.F. Stoddart, Org. Lett. 6 (2004) 4167.
[65] S.A. Vignon, J. Wong, H.-R. Tseng, J.F. Stoddart, Org. Lett. 6 (2004) 1095.
[66] B. Moulton, M.J. Zaworotko, Chem. Rev. 101 (2001) 1629.
[67] M.J. Rosseinsky, Micropor. Mesopor. Mater. 73 (2004) 15.
[68] M. Eddaoudi, D.B. Moler, H. Li, B. Chen, T.M. Reineke, M. O'Keeffe, O.M. Yaghi, Acc. Chem. Res. 34 (2001) 319.
[69] S.L. James, Chem. Soc. Rev. 32 (2003) 276.
[70] D. Maspoch, D. Ruiz-Molina, K. Wurst, N. Domingo, M. Cavallini, F. Biscarini, J. Tejada, C. Rovira, J. Veciana, Nat. Mater. 2 (2003) 190.
[71] G.J. Halder, C.J. Kepert, B. Moubaraki, K.S. Murray, J.D. Cashion, Science 298 (2002) 1762.
[72] X.-H. Bu, M.-L. Tong, H.-C. Chang, S. Kitagawa, S.R. Batten, Angew. Chem. Int. Ed. 43 (2003) 192.
[73] B. Chen, N.W. Ockwig, A.R. Millward, D.S. Contreras, O.M. Yaghi, Angew. Chem. Int. Ed. 44 (2005) 4745.
[74] J.L.C. Rowsell, O.M. Yaghi, Micropor. Mesopor. Mater. 73 (2004) 3.
[75] J.L.C. Rowsell, O.M. Yaghi, Angew. Chem. Int. Ed. 44 (2005) 4670.
[76] C. Janiak, Dalton (2003) 2781.
[77] W. Lin, J. Solid State Chem. 178 (2005) 2486.
[78] P. Diaz, J. Benet-Buchholz, R. Vilar, A.J.P. White, Inorg. Chem. 45 (2006) 1617.
[79] M.J. Plater, B.M. de Silva, J.M.S. Skakle, R.A. Howie, A. Riffat, T. Gelbrich, M.B. Hursthouse, Inorg. Chim. Acta 325 (2001) 141.
[80] M.J. Hannon, C.L. Painting, E.A. Plummer, L.J. Childs, N.W. Alcock, Chem. Eur. J. 8 (2002) 2225.
[81] K.S. Min, M.P. Suh, J. Am. Chem. Soc. 122 (2000) 6834.
[82] A.N. Khlobystov, A.J. Blake, N.R. Champness, D.A. Lemenovskii, A.G. Majouga, N.V. Zyk, M. Schroder, Coord. Chem. Rev. 222 (2001) 155.
[83] C. Inman, J.M. Knaust, S.W. Keller, Chem. Commun. (2002) 156.
[84] S. Lopez, S.W. Keller, Inorg. Chem. 38 (1999) 1883.
[85] A.J. Blake, N.R. Champness, P.A. Cooke, J.E.B. Nicolson, C. Wilson, Dalton (2000) 3811.
[86] A.J. Blake, G. Baum, N.R. Champness, S.S.M. Chung, P.A. Cooke, D. Fenske, A.N. Khlobystov, D.A. Lemenovskii, W.-S. Li, M. Schroder, Dalton (2000) 4285.
[87] D.L. Reger, R.F. Semeniuc, V. Rassolov, M.D. Smith, Inorg. Chem. 43 (2004) 537.

[88] D.L. Reger, R.P. Watson, J.R. Gardinier, M.D. Smith, Inorg. Chem. 43 (2004) 6609.
[89] L. Yi, X. Yang, T. Lu, P. Cheng, Cryst. Growth Des. 5 (2005) 1215.
[90] H.-J. Kim, W.-C. Zin, M. Lee, J. Am. Chem. Soc. 126 (2004) 7009.
[91] M.J. Whitcombe, C. Alexander, E.N. Vulfson, Synlett (2000) 911.
[92] J. Steinke, D.C. Sherrington, I.R. Dunkin, Adv. Polym. Sci. 123 (1995) 81.
[93] Y. Kanekiyo, K. Inoue, Y. Ono, M. Sano, S. Shinkai, D.N. Reinhoudt, J. Chem. Soc. Perkin Trans. 2 (1999) 2719.
[94] P. Turkewitsch, B. Wandelt, G.D. Darling, W.S. Powell, Anal. Chem. 70 (1998) 2025.
[95] J.-q. Liu, G. Wulff, Angew. Chem. Int. Ed. 43 (2004) 1287.
[96] J.-q. Liu, G. Wulff, J. Am. Chem. Soc. 126 (2004) 7452.
[97] R.L. Simon, D.A. Spivak, J. Chromatogr. B 804 (2004) 203.
[98] L. Wu, Y. Li, Anal. Chim. Acta 517 (2004) 145.
[99] D. Guillon, B. Donnio, D.W. Bruce, F.D. Cukiernik, M. Rusjan, Mol. Cryst. Liq. Cryst. 396 (2003) 141.
[100] T. Chuard, R. Deschenaux, J. Mater. Chem. 12 (2002) 1944.
[101] N.V. Madhusudana, Curr. Sci. 80 (2001) 1018.
[102] F.J.M. Hoeben, P. Jonkheijm, E.W. Meijer, A.P.H.J. Schenning, Chem. Rev. 105 (2005) 1491.
[103] M. Imperor-Clerc, Curr. Opin. Colloid Interface Sci. 9 (2005) 370.
[104] D. Kim, S. Jon, H.-K. Lee, K. Baek, N.-K. Oh, W.-C. Zin, K. Kim, Chem. Commun. (2005) 5509.
[105] Y.R. De Miguel, J.K.M. Sanders, Curr. Opin. Chem. Biol. 2 (1998) 417.
[106] R.L.E. Furlan, S. Otto, J.K.M. Sanders, Proc. Natl. Acad. Sci. U.S.A. 99 (2002) 4801.
[107] S. Otto, R.L.E. Furlan, J.K.M. Sanders, Science 297 (2002) 590.
[108] S. Otto, R.L.E. Furlan, J.K.M. Sanders, Drug Discov. Today 7 (2002) 117.
[109] J.-M. Lehn, Chem. Eur. J. 5 (1999) 2455.
[110] J.-M. Lehn, A.V. Eliseev, Science 291 (2001) 2331.
[111] O. Ramstrom, J.-M. Lehn, Nat. Rev. Drug Discov. 1 (2002) 26.
[112] S.J. Rowan, S.J. Cantrill, G.R.L. Cousins, J.K.M. Sanders, J.F. Stoddart, Angew. Chem. Int. Ed. 41 (2002) 899.
[113] S. Otto, S. Kubik, J. Am. Chem. Soc. 125 (2003) 7804.
[114] S.G. Telfer, X.-J. Yang, A.F. Williams, Dalton Trans. (2004) 699.
[115] L.P. Harding, J.C. Jeffery, T. Riis-Johannessen, C.R. Rice, Z. Zeng, Chem. Commun. (2004) 654.